

**FLOOD HAZARD EVALUATION AND
FOUNDATION RECOMMENDATIONS
BORREGO SPRINGS SUBDIVISION
APN 141-080-05
BORREGO, CALIFORNIA**

Prepared for
KRS Development, Inc.
401(K) Retirement Savings Plan (002)
FBO Kent R. Smith
San Marcos, California



Prepared by
TERRACOSTA CONSULTING GROUP, INC.
San Diego, California

Project No. 2418
August 2, 2006



Geotechnical Engineering

Coastal Engineering

Maritime Engineering

Project No. 2418
August 2, 2006

KRS Development, Inc.
401(K) Retirement Savings Plan (002)
FBO Kent R. Smith
1578 Palomar Drive
San Marcos, California 92069

FLOOD HAZARD EVALUATION AND
FOUNDATION RECOMMENDATIONS
BORREGO SPRINGS SUBDIVISION
APN 141-080-05
BORREGO, CALIFORNIA

Gentlemen:

TerraCosta Consulting Group, Inc. (TCG) is pleased to provide this report, which presents the results of our hydraulic and flood hazard study, and their affect on your proposed development. We have also provided preliminary foundation design criteria for residential construction consistent with the County of San Diego's Borrego Valley Flood Management Report.

The subject 50-acre property spans a good portion of Hellhole Canyon, the entirety of Fire Canyon, and the southerly portion of Borrego Palm Canyon, with flood waters from at least the southerly two alluvial drainages passing through the property. We have also superimposed the proposed 50-acre development on the County's Flood Hazard Map for Borrego Valley contained in the County's Borrego Valley Flood Management Report, a portion of which is reproduced in the accompanying report.

As a contributing author of the original Borrego Valley Flood Management Report and the principal investigator/author of the Technical Basis for Design of Structural Improvements for the Borrego Valley Flood Control Master Plan

(Appendix 3 of the County's Flood Management Report), we can offer that in 1989, it was envisioned that the Flood Management Report would help facilitate and encourage flood management guidelines for very limited-growth rural development in the Borrego Valley through a variety of non-structural flood plain management techniques. Where more urban development was proposed, it was also envisioned that the Flood Management Report would help facilitate and encourage the developer to work with both the County and the downstream property owners in effectively passing flood flows through and/or around the urban areas without adversely affecting downstream property owners and neighboring properties along the same contour within a given alluvial fan boundary. Ultimately, it was and remains the County's desire to safely pass the flood flows down the various canyons with a minimum of disruption to both private property and public infrastructure through the fan terminus alluvial wash and ultimately down to the Borrego Sink.

In Appendix 5 of the Borrego Valley Flood Management Report, a wide variety of structural flood control alternatives were investigated for reducing flood flows in Coyote Creek, Henderson Canyon, Borrego Palm Canyon, Hellhole Canyon, and Tubb Canyon. Of the eleven alternatives discussed in the Flood Management Report, five were devoted to the Borrego Palm Canyon / Hellhole Canyon study area, with significant technical background provided for Borrego Palm Canyon as the basis for designing any future structural channelization projects throughout the valley. Moreover, the Borrego Palm / Fire / Hellhole Canyon complex currently floods the most urbanized area of the valley, with considerable attention given to these three coalescing alluvial fans, all of which also affect the subject property.

As the principal author of the Technical Basis of Design for Structural Improvements for the Borrego Valley Flood Control Master Plan and, as this document describes in some detail the hydraulics specific to Borrego Palm Canyon, we have reproduced portions of the technical appendix specific to Borrego Palm Canyon to provide additional insight into the flood hazards within the upper reaches of these coalescing alluvial fans, and to provide additional

technical basis for the proposed foundation design criteria, consistent with the County's Flood Management Report guidelines.

We appreciate the opportunity to be part of your design team for this project. If you have any questions or require additional information, please give us a call.

Very truly yours,

TERRACOSTA CONSULTING GROUP, INC.



Walter F. Crampton, Principal Engineer
R.C.E. 23792, R.G.E. 245

WFC/jg
Attachments

- (2) Addressee
- (5) Ms. Jo MacKenzie, The MacKenzie Group
- (1) Mr. Mark Stevens, Stevens-Cresto Engineering



TABLE OF CONTENTS

1	PROPOSED PROJECT	1
2	DESCRIPTION OF STUDY AREA.....	2
3	BORREGO VALLEY SPECIAL FLOOD HAZARDS	3
4	SEDIMENT TRANSPORT CAPACITY.....	7
5	THE BORREGO VALLEY REGIME EQUATION MODELS	11
6	DESIGN CONSIDERATIONS	14
6.1	Evaluation of Available Regime Equations	15
7	PIER SCOUR.....	18
7.1	Scour from Debris on Piers	20
7.2	Width of Scour Holes	21
8	FOUNDATION DESIGN RECOMMENDATIONS	24
8.1	Lateral Pier Capacity	24
8.2	Axial Pier Capacity	26
8.3	Alternative Foundation Types	26

REFERENCES

TABLE 1 - REGIME CHARACTERISTICS OF STREAM CHANNELS

TABLE 2 - REGIME RELATIONS FOR VARIOUS RIVERS

- FIGURE 1 - SITE PLAN
- FIGURE 2 - TENTATIVE PARCEL MAP (prepared by Stevens-Cresto Engineering)
- FIGURE 3 - REGIME CONDITIONS
- FIGURE 4 - SEDIMENT DISCHARGE FOR COLORADO RIVER
- FIGURE 5 - SEDIMENT DISCHARGE AS A FUNCTION OF WATER DISCHARGE
- FIGURE 6 - SEDIMENT DISCHARGE AS A FUNCTION OF SLOPE
- FIGURE 7 - THE RELATIONSHIP OF Φ VS α
- FIGURE 8 - SEDIMENT DISCHARGE CURVES FOR VARIOUS REGIME METHODS

APPENDIX A - CALCULATIONS

APPENDIX B - DEBRIS LOADING DESIGN CRITERIA

APPENDIX C - FOUNDATIONS AND EARTH STRUCTURES, NAVFAC DM 7.02

FLOOD HAZARD EVALUATION AND
FOUNDATION RECOMMENDATIONS
BORREGO SPRINGS SUBDIVISION
APN 141-080-05
BORREGO, CALIFORNIA

1 PROPOSED PROJECT

The proposed 50-acre development lies adjacent to and westerly of Hoberg Road, just north of Palm Canyon Drive on the western flanks of the Borrego Valley in eastern San Diego County, California. The development extends from Palm Canyon Drive northerly a distance of approximately 3,680 feet and extends westerly for a distance of approximately 600 feet to the easterly boundary of the Anza Borrego Desert State Park. The southerly 920 feet of this relatively long and narrow parcel has been set aside for a future commercial site, with the northerly 2,760-foot parcel proposed for thirty-three 1-acre minimum residential sites, with loop access off Hoberg Road.

The 50-acre property spans the majority of Hellhole Canyon, the entirety of Fire Canyon, and the southerly portion of Borrego Palm Canyon, with flood waters from at least the southerly two alluvial drainages passing through the property. We have also superimposed the proposed 50-acre development on the County's Flood Hazard Map for Borrego Valley contained in the County's Borrego Valley Flood Management Report, a portion of which is reproduced herein as the Site Plan, Figure 1.

Figure 1 also shows the alluvial fan boundaries and the depth-velocity lines for use in designing flood protection improvements on these alluvial fans, as provided in the County's Flood Management Report. Also shown on Figure 1 are the eastern limits of the State Park boundaries, which abut up to the western property line of the subject property.

The Tentative Parcel Map prepared by Stevens-Cresto Engineering is included as Figure 2. As indicated on both Figures 1 and 2, site topography is primarily controlled by the Hellhole alluvial fan, with average gradients passing through the

site on the order of 3.3 percent. Proposed site improvements are relatively limited and are confined to at-grade asphalt concrete driveways and underground utilities. Recognizing that these one-acre lots are near the mouth of Hellhole Canyon and Fire Canyon, the proposed residential improvements will be limited to pier-supported elevated structures capable of passing the 100-year flood flows beneath the elevated structural first floor of the residences. The piers supporting the elevated structures must also be designed to accommodate scour around the piers resulting from the presence of the pier within the floodway. Similarly, at-grade asphalt concrete driveways will require sufficient cut-off walls and/or thickened edges to preclude flood-induced undermining and damage to the access driveways.

2 DESCRIPTION OF STUDY AREA

The Borrego Valley is bounded by relatively rugged granitic terrain on all quadrants, with all drainage flowing to the Borrego Sink located near the southeasterly edge of the valley, and thereafter discharging to the east through the Borrego Sink Wash. The valley itself has been formed by alluvial processes from Coyote Creek, which trends in a southeasterly direction and is fed by a 137-square-mile upland watershed. The alluvial fan, developed from the Coyote Creek watershed, is the predominant geomorphic feature within the valley and controls virtually the entire topography of the valley. Seven recognizable alluvial fans are incised into the relatively rugged crystalline terrain to the west, often coalescing with an adjacent fan a short distance down into the valley. Borrego Palm Canyon, Fire Canyon, and Hellhole Canyon represent the central western portion of the valley side slopes, with these three canyons having drainage areas of 25 square miles, 0.7 square mile, and 12.5 square miles, respectively. Hundred-year design flood flows for these three canyons are 11,700 cfs, 4,000 cfs, and 7,700 cfs respectively. The County typically combines the Fire Canyon and Hellhole Canyon 100-year design flows for any projects downstream of the confluence of these two canyons, which would clearly be appropriate for the subject site.

3 BORREGO VALLEY SPECIAL FLOOD HAZARDS

Design floods in the Borrego area are based upon summer tropical storms of brief duration and extreme intensity. Sizeable floods have occurred in recent years in the Borrego area and most of the flooding has taken place in the summer and fall months from local thunderstorms and tropical cyclones generated in the south Pacific and Gulf of Mexico. During these severe storms, large quantities of overland flow develop in the sparsely vegetated granitic mountains that surround Borrego Valley. The surface runoff collects in narrow steeply walled canyons, and upon reaching the canyon mouth, the unconfined water spreads into sheet flow across the wider alluvial surfaces.

Upon reaching the alluvial fan, the permeability of the active channel bed changes from relatively impervious (representative of the steep, mountainous upland section) to highly pervious alluvial sands and gravels which comprise the planar surface of the fan. These relatively clean alluvial deposits have initial infiltration rates upwards of 1 inch of rainfall in 3 to 5 seconds (Group Delta Consultants, 1988). These substantial infiltration losses further complicate an evaluation of flood flows moving downgradient on the fan due to the non-steady-state discharge characteristics of the flood flow.

Topographically, the alluvial fans originate as relatively steep deltaic features emanating from the mouths of canyons, and become progressively flatter as they approach the lower valley floor. The upper reaches of the fans are largely confined to wide arroyos or fanhead trenches. This area is often referred to as the channelized flow zone and is characterized by a single entrenched channel cut into the head of the fan. Depending upon the available upland sediment supply, this typically degrading zone may occasionally aggrade, resulting in a more random flow even near the head of the fan. A good description of fanhead entrenchment is provided by Schumm and others (1987). Continuing downslope, the washes widen into a complex braided pattern of active and inactive courses. These channels are generally confined by low, near-vertical banks that are easily breached, diverting flood stage runoff into sheet flow across the desert floor.

Important to an understanding of alluvial fan hydraulics is that flood flows on an alluvial fan are not typically constrained to a given flow width, and they tend toward a dynamic equilibrium to most efficiently accommodate the sediment-laden flood flows transiting the fan. This essentially means that, although flood flows down the face of the fan can have a relatively high transport capacity, as long as sufficient sediment yield is supplied by the watershed, a state of stream equilibrium can be maintained, which results in neither erosion nor deposition of sediment. In order to evaluate the aggradation and degradation within a reach of a stream bed or the less constrained alluvial fan, it is necessary to divide the reach into several sections and calculate the sediment transport into and out of a given section. Streams tend to aggrade or degrade in discrete reaches. The process alternates between aggradation and degradation as the flow passes from one reach to the next. The rate at which aggradation or degradation takes place depends upon the sediment yield, the grain size of sediment particles, and the stream discharge. These discrete reaches are not fixed in space. They tend to shift back and forth with respect to time, magnitude of water discharge, and land-use changes.

The process of sedimentation can be described mathematically as follows (Lane, 1955; Chang, 1988, pg. 28, eq. 2.30):

$$(\text{sediment discharge}) \times (\text{sediment size}) \propto (\text{stream slope}) \times (\text{stream discharge})$$

For example, if a river has a certain water discharge with a stabilized sediment grain size distribution, which has been developed after a number of years, the channel will establish its slope, cross-sectional shape, and flow pattern to most efficiently accommodate the flow. The channel will remain in equilibrium by adjusting any one of the above parameters in response to changes in the stream flow.

Examination of the previous relationship leads to the conclusion that ephemeral (intermittent) streams never attain a true state of equilibrium. The discharge changes drastically from little or no flow most of the year, to large flood flows for a short duration. Ephemeral streams are constantly changing in response to the very erratic, short-duration, high-intensity flood flows that pass through them.

Researchers have recognized that unconstrained flood flows down alluvial fans, and within all natural streams for that matter, tend toward an equilibrium or regime flow condition, which can be numerically described in a general form for width, depth, and flow velocity (Leopold and Maddock, 1953).

These equations are given by:

$$\begin{aligned} B &= \Phi Q^{\alpha} \\ D &= \Delta Q^{\delta} \\ V &= \Omega Q^{\omega} \end{aligned}$$

Where:

$$\begin{aligned} B &= \text{flow width} \\ D &= \text{flow depth} \\ V &= \text{flow velocity} \\ Q &= \text{flow volume} \end{aligned}$$

Due to the principle of continuity, it follows that:

$$(BD)V = Q = (\Phi Q^{\alpha} \Delta Q^{\delta}) \Omega Q^{\omega}$$

and

$$\begin{aligned} \alpha + \delta + \omega &= 1 \\ \Phi \Delta \Omega &= 1 \end{aligned}$$

Since we are primarily interested in the regime width of flow, which in turn affects the total sediment transport capacity of a given volume of flow crossing the alluvial fan, we will concentrate on the general width equation. Although described in significantly more detail in the Technical Appendix to the Borrego Valley Flood Control Master Plan, the exponent α is primarily a function of the channel bed's natural tendency to resist erosion with higher values indicating more easily erodible soil, and lower values indicating less erodible soils. Both α and Φ are functions of the specific watershed characteristics and cannot be implicitly solved for, given the

characteristics of the Borrego Valley watershed. However, α is a function of Φ and, as discussed in the Technical Appendix, regime equations for flow widths on alluvial fans have been developed for southern California conditions and are appropriate for the Borrego Valley.

The three regime equations cited in the Technical Appendix follow:

$$W = 2.54Q^{0.65} \quad \dots \quad \text{Rams Hill}$$

$$W = 9.5Q^{0.4} \quad \dots \quad \text{Dawdy}$$

$$W = 17.2(Qn)^{3/8} / S^{3/16} \quad \dots \quad \text{Cabazon}$$

The Rams Hill equation developed by this author was for the upper reaches of the alluvial bajada (a series of discrete coalescing alluvial fans) just east of Yaqui Pass Road, where the gradient on the alluvial floor was approximately 5 percent. The Dawdy equation developed by David Dawdy (1979), originally for FEMA in developing their flood hazard actuarials, is currently in use throughout the arid southwest. Moreover, Dr. Dawdy was retained by the County of San Diego to review the procedures outlined in the Borrego Valley Flood Management Report, and it was his conclusion that his regime equation was well suited for Borrego Valley and particularly on the lower slopes of the valley. The Cabazon method was developed for the community of Cabazon in Riverside, California, by PRC Toups in 1980, and essentially mirrors the Dawdy equation. Regime widths obtained from the three equations, along with other hydraulic parameters, are shown on Figure 3.

Important to this preceding discussion is the regime width for a given flood flow beyond which any channel widening is unlikely. This again is due to the conservation of energy, recognizing that a progressively wider channel requires more energy to convey a given amount of sediment-laden flood waters. The Rams Hill equation, although indicating a somewhat wider regime width, was developed for a condition having a slightly steeper valley floor slope (5 percent) than the 3.3 percent slope passing through the subject property.

As a practical matter, however, what drives stream bed degradation or aggradation within a discrete reach is the potential for channel confinement, which locally accelerates flood waters, increasing sediment transport capacity and degradation potential. This, of course, occurs with elevated building pads within the floodway and is more severe when using the Dawdy or Cabazon models.

4 SEDIMENT TRANSPORT CAPACITY

The configuration and characteristics of an alluvial channel are influenced most by the sediment balance of the system, i.e., the relationship between the sediment transport capacity of the flowing water and the available sediment. Sediment transport itself is influenced by the complex interrelationship of several parameters including the grain size, density, shape and cohesiveness of the bed and bank material of the channel; the geology, hydrology, meteorology, topography, soils, and vegetative cover of the drainage basin; and the width, velocity, slope, temperature and turbulence of the flowing water. A change or alteration in one parameter will be followed by changes in others. Alluvial systems are dynamic in nature, continually seeking a new equilibrium condition in response to changes in flow.

In order to understand the processes of aggradation and degradation in free-flowing streams, an understanding of the mechanisms of sediment transport is necessary. When a liquid starts moving, hydrodynamic forces are exerted on the solid particles of the bed along the wetted surface of the channel or river. An increase in the flow intensity creates an increase in the magnitude of these forces. Hence, for a channel bed composed of noncohesive sandy soil, a flow condition will be reached at which particles in the bed are unable to resist the hydrodynamic forces, and are dislodged and eventually will start to move along the channel bottom. One method for evaluating transport capacity is to evaluate the bed shear stress, which is a function of water depth and channel slope, and compare that to the critical shear stress (tractive force), which is a function of particle geometry, and, at higher flow rates, the sediment transport rate. For a given flow condition, the difference between the

bed shear stress and the critical shear stress provides a factor for evaluation of sediment transport capacity.

Numerous equations exist for calculation of the sediment transport capacity of a given stream. Equations have been developed to calculate the suspended or wash load, the bed load, and the total sediment load within a stream. Other things being equal, the transport capacity of the bed load increases with increase in suspended load (due to increased bed shear stress). However, due to the hard rock terrain which surrounds the Borrego Valley, only limited suspended load is produced from the watershed. Sand size particles, which make up the bed load, are the predominant source material for aggradation and degradation in fairly high energy alluvial environments. As such, we have limited our evaluations to the bed load type of equations. There are essentially three different approaches to evaluating the bed load within an alluvial stream. They are (1) the DuBoys-type equations, which consider the shear stress relationships; (2) the Schoklitsh-type equations, which evaluate the velocity and discharge relationships within a given channel section; and (3) the Einstein-type equations which are based on statistical considerations of the lift forces.

As can be seen on Figure 4, each of the various sediment discharge formulae may yield variations in sediment discharge of several orders of magnitude (Vanoni and others, 1977, pg. 221), making it difficult to select a formula for analyzing a particular problem. Each formula has been developed to model a particular set of data and may be considered appropriate for similar conditions. Many of the formulae presented in the literature were developed for canals that typically have slopes ranging from 0.0001 to 0.001 feet per foot. Figure 5 depicts the sediment discharge relationship using six different formulae given a channel slope of 4 percent. Figure 6 depicts the range in sediment discharge using the same six equations given a constant flow rate and varying the channel slope from 0.0001 to 0.1 feet per foot.

The sediment transport capacity equations become more complicated when dealing with supercritical flow. Most of the flume data used to formulate the earlier equations, such as the DuBoys and the Shields equations, were limited to only

subcritical flow. Several of the authors, such as Ackers-White (1973), indicate that their formulae have not been tested for supercritical flow regimes. The formula developed by Engelund-Hansen (1967) has been developed for both subcritical and supercritical flow and reportedly produces good results.

The selection of the most appropriate bed load capacity formulae is complicated by the fact that the results of different formulae differ substantially and it is uncertain as to which one gives the most realistic result. Items such as temperature, viscosity, flow velocity, specific density of the fluid and sand particles and variations in particle size affect the transport capacity of an alluvial stream. By varying particular parameters, the discharge relationships would vary somewhat from those shown on Figures 4, 5, and 6. The six equations used to produce Figures 5 and 6 are presented and discussed in some detail in the Technical Appendix. It was ultimately concluded that the Engelund-Hansen equation was most appropriate for modeling supercritical flood flows in the Borrego Valley.

The transport capacity of the alluvial stream is further complicated by the changes in flow resistance associated with the changes in bed form caused by changes in the stream power, $\tau_o v = \gamma R S V$ (Chang, 1988). Selection of the roughness coefficients is likewise complicated when dealing with shallow flow due to the increased effect of surface roughness relative to the hydraulic radius.

A close examination of the equations reveals that changes in channel width result in sizeable variations in the sediment transport capacity. In other words, relatively narrow channels are considerably more efficient and hence have higher sediment transport capacities than the less efficient wider and shallower channel. Depending on the formula used, variations in sediment transport capacity could amount to a five-fold increase with a ten-fold decrease in the channel width. The importance of this concept becomes quite clear when we examine alluvial fans in which almost all storm runoff occurs as sheet flow, confined to only a small portion of the relatively steep alluvial fan.

In order to use the general regime equations, it is necessary to evaluate the constants Φ , Δ , and Ω . Unfortunately, these constants are a function of the specific watershed characteristics and cannot be implicitly solved for, given the characteristics of the Borrego Valley watershed. Fairly large variations in these constants exist when comparing the available information in the literature. Table 1 provides a summary of both Φ and α for the 20 stream channels studied by Leopold and Maddock (1953). For the streams studied, α appears to be a function of Φ , and this relationship is illustrated in Figure 7.

Table 2 provides a summary of the values obtained for the three exponents from natural streams and rivers by several different researchers (Graf, 1971, pg. 255). Regime formulas developed by Russian researchers have determined that α equals 0.57 (Kondrat'ev and others, 1959; Chang, 1988, pg. 22). On the basis of flume studies, it has been determined that α equals 0.9 for truly cohesionless sands (Wolman and Brush, 1961).

It should be noted that the data presented in Table 1 and Figure 7 represent generalized regime conditions for natural streams which are not ephemeral and, admittedly, somewhat different than an alluvial fan. Data on alluvial fans is somewhat sparse at best, and most researchers continue to model alluvial fan hydraulics based on the available regime data. As such, there is a natural tendency to limit flow widths and, hence, increase the unit discharge on the fan. This has a rather significant effect on the scour potential and computed bed load capacity. In general, higher α values result in a greater width of unconfined regime flow down the fan and a lower unit sediment discharge rate. It is interesting to note that alluvial fans in the Death Valley region of California and Nevada have a headland watershed between 1 and 30 square miles, and a relatively uniform slope ranging between 4.5 and 17 percent (no trends, just average scatter values). For these conditions, the width of the active wash or channel sampled along seven washes in the Death Valley region ranged between 400 and 6,000 feet (Denny, 1965). Although no attempt was made to determine the regime coefficients for width of the active wash, it is interesting to note the major variations in flow width that develop on steeply braided alluvial fans.

In general, the α coefficient provides an indicator of the relative cohesiveness of the material exposed in the banks of a channel, acknowledging that an upper limit, i.e. purely cohesionless coarse-grained sands, would have an α value of 0.9, and a nonerodible channel would have an α value of zero (0). As reported in Table 1, α values measured by Leopold and Maddock ranged from 0.3 (very little change in flow width, with increase in discharge) to 0.59 (large increase in flow width, with increase in discharge).

As can be seen from Table 2, an α coefficient in excess of 0.5 seems appropriate for alluvial fans in the Borrego Valley, realizing that 0.9 would be an upper limit. One can argue that, since most ephemeral streams in the arid southwest United States typically have some natural cementation on the side slopes of the bank, exponents of 0.5 may be somewhat low for the Borrego Valley. Admittedly, alluvial fans generally consist of noncohesive sandy soils having little or no fines; however, the presence of vegetation tends to provide artificial cementation which in turn would tend to limit horizontal development of a particular stream channel. The α coefficient used in the design of the flood control improvements at Rams Hill was 0.65 based on this hypothesis and the regime equation was calibrated using existing geomorphic features in the site vicinity (Woodward-Clyde Consultants, 1982).

5 THE BORREGO VALLEY REGIME EQUATION MODELS

As part of the perimeter flood control design for the Rams Hill Development, Woodward-Clyde Consultants (WCC) staff conducted site surveys of the braided upper reaches of the alluvial fan where localized geologic constrictions forced fairly uniform sheet flow just upstream of these constructions, thus enabling back-calculations of the available capacity within the several braided channels. These calculations allowed calibration of the general regime equation for width as a function of flow for hydraulic conditions unique to the Rams Hill site. A detailed discussion of the calibration approach can be found in WCC's referenced documents. For the Rams Hill development, the design regime equation for width is as follows:

$$W = 2.54Q^{0.65} \quad \dots \quad \text{Rams Hill}$$

Two other regime equations have been considered in development of the design criteria for structural improvements within the Borrego Valley. Namely, the equation developed by Dawdy (1979) and the equation developed for the community of Cabazon in Riverside, California (PRC Toups, 1980). Equations for the regime width using these two methods are as follows:

$$\begin{aligned} W &= 9.5Q^{0.4} && \dots \quad \text{Dawdy} \\ W &= 17.2 (Qn)^{3/8} / S^{3/16} && \dots \text{Cabazon} \end{aligned}$$

The Dawdy method was designed primarily for use in flood frequency estimates on alluvial fans which have subsequently been adopted by the Federal Emergency Management Agency, FEMA. Dawdy made the assumption that flow on the fan maintains critical depth and velocity and that the channel stabilizes approximately at a point where $dD/dW = -0.005$. By taking the first derivative of D with respect to W and setting this value equal to -0.005 , one arrives at the equation $W = 9.5Q^{0.4}$. Although other investigators have criticized the Dawdy method (McGinn, 1980), it does provide a computational method for assigning a flood hazard to a given site for subsequent use in writing flood insurance policies. Since policies are, in part, set by actuarials, the Dawdy method does a good job at fulfilling the basic needs of FEMA. It should be pointed out, however, that the α coefficient of 0.4 may be somewhat low for the alluvial fans within the Borrego Valley and, therefore, the computed unit transport capacity at a given site may be unrealistically high. This requires a conservatively designed structure to mitigate channel bed scour in the vicinity of a structure.

The Cabazon method is a derivative of the Dawdy method, with the assumption made that the Manning's resistance equation is more appropriate than the critical depth used by Dawdy. The Cabazon method also assumes that the width-depth ratio stabilizes at 200. Thus, by equating this to the first order derivative of depth with respect to width using Manning's equation, one obtains the regime width equation developed by PRC Toups.

The Cabazon method provides an interesting dilemma in that one must now select a Manning's n-value in order to compute the regime width. As one can imagine, relatively low n-values (say on the order of 0.025 to 0.035) would result in substantially larger computed sediment discharge rates than those obtained by the Dawdy method (this actually varies with the bed load equation used). The Cabazon study used n-values of 0.035, which resulted in relatively narrow regime channel widths and relatively high flow velocities; substantially higher than what would have been obtained using the Dawdy method. As before, the same comments would apply to the Cabazon method. Of the three methods, the Cabazon method is most likely to result in streambed degradation when confined by any structures or elevated building pads. The Rams Hill method would be most likely to cause stream bed aggradation for the same channel construction.

The Dawdy method and the Cabazon method both assume that the channel stabilizes at a width-depth ratio of 200. Dawdy admits that this is based on his personal communication with Boyd Lare, U.S. Army Corps of Engineers, in 1978. Admittedly, most of the literature referencing regime flow conditions cites width-depth ratios of less than 200. It is important to note that, with the exception of the Denny (1965) data, virtually no information is available regarding the regime flow width down alluvial fans. Leopold and Miller (1956) recorded width-depth ratios upwards of 400 on the Canada Ancha, near El Rancho Montoso, an arroyo in New Mexico. Moreover, they measured Froude numbers on the order of 1.5 during estimated peak flows. This, of course, is at variance with the Dawdy method. It is also interesting to note that, for this arroyo, $\Phi \approx 13.1$ and $\alpha = 0.39$.

Some controversy still exists between various researchers regarding the flow regime of alluvial fans (Dawdy, 1979; PRC Toups, 1980; French, 1984; Schumm and others, 1987; Chang, 1988). Regime flow on alluvial fans is considered to be either supercritical or critical. For critical flow to occur, the equivalent Manning's n-value must approach 0.1, which results in relatively deep flow depths; a feature not typically observed on alluvial fans. Critical flow combined with high width-depth ratios results in the lowest possible computed value of sediment discharge delivered to a structure. Critical flow and narrow width-depth ratios (the Dawdy method)

provide somewhat higher computed sediment discharge values at a structure. Supercritical flow (assuming n -values of 0.025 to 0.035) and narrow regime flow widths (the Cabazon method) generate the highest computed sediment discharge values at a structure (depending upon the bed load equation used). The actual effects of these different assumptions are illustrated on Figure 8 and described in more detail in the following section.

6 DESIGN CONSIDERATIONS

When designing a structure sited on an alluvial fan, whether intended to convey sediment-laden flood waters through urbanized areas or to simply protect other improvements in or adjacent to the structure, one must balance the sediment transport capacity, through or around the structure, to that value delivered to the structure. This is especially true for channels with armored banks and erodible beds, where a substantial change in transport capacity could cause substantial erosion and damage to the structure if the transport capacity in or around the structure were increased relative to the upgradient transport capacity. Similarly, a reduction in transport capacity could cause the structure to fill in, overtopping the structure with uncontrolled sediment-laden flood waters then breaching the structure, likely to the detriment of downgradient improvements.

As indicated on Figures 4 and 5, for a given slope, sediment transport capacity is a function of the flood water discharge and is typically expressed in terms of pounds per second per foot. With alluvial fans, the selection of a regime equation then becomes an important factor, as a relatively wide regime width results in a relatively low unit flood water discharge, with a corresponding low sediment discharge. To properly model the effect of structures, and particularly structures on the upper reaches of an alluvial fan, use of the proper regime model is important when sizing structural improvements.

The County's Flood Management Report addressed in some detail the hydraulics specific to Borrego Palm Canyon immediately downstream of Hoberg Road to illustrate the structural design requirements necessary for sizing a flood control

channel through that area, capable of accommodating both the flood flow and sediment flow, while minimizing the streambed degradation or aggradation. The sediment discharge rates were based on the DuBoys, Engelund-Hansen and Ackers-White bed load equations, with the results as follows:

6.1 Evaluation of Available Regime Equations

$$W = 9.5Q^{0.4} \quad \dots \text{Dawdy Method}$$

$$W = 17.2(Qn)^{3/8} / S^{3/16} \quad \dots \text{Cabazon Method}$$

$$W = 2.54Q^{0.65} \quad \dots \text{Rams Hill Method}$$

Using Borrego Palm Canyon as an example, the design hydraulic properties are as follows:

$$Q_{100} = 11,700 \text{ cfs}$$

$$S = 2\frac{1}{2}\% \text{ (in the vicinity of the inlet to the County's proposed Borrego Palm Canyon flood control structure)}$$

$$n = 0.025$$

Method	Regime Width (feet)	Flow Depth (feet)	Bed Load Equation						Froude No.	Velocity (ft/sec)
			DuBoys		Engelund-Hansen		Ackers-White			
			Q _s (#/sec)	q _s (#/sec/ft)	Q _s (#/sec)	q _s (#/sec/ft)	Q _s (#/sec)	q _s (#/sec/ft)		
Dawdy	402.7	2.97	237,985	591	125,037	311	2,878	7	1.0	9.78
Cabazon	288.9	2.39	110,346	382	187,269	648	8,970	31	1.93	16.94
Rams Hill	1129.8	1.05	84,547	75	73,873	65	8,384	7	1.70	9.86

It should be noted that the effect of using vastly different Q_s values at the inlet to a structure is not as significant as one might initially think since the same bed load equation is then used to size the structure. Additionally, as can be seen, the use of an $\alpha = 0.65$ and a very high width-depth ratio does not necessarily imply that one is using a liberal design philosophy. This initial step merely provides the input into the channel, which then allows one to size the channel and evaluate its

tendency to either aggrade or degrade. Simply stated, the most realistic model should provide the designer with the best information.

The implication of the preceding table is more problematic for the proposed development in that the 33 proposed 1-acre residential lots, when measured along the contour, have a typical dimension on the order of 250 to 300 feet and, thus, if either the Dawdy or Cabazon method properly models the regime conditions, the entire design storm from any flood flows originating from Hellhole/Fire Canyon or Borrego Palm Canyon could, worst case, pass through a single lot. If, for example, one were to build an elevated pad covering less than 25 percent of the lot area, as envisioned by the County's Flood Management Report, this 10,000-square-foot pad could easily block from 30 to 50 percent of the design flood flow, with stagnation pressures resulting in upwards of several hundred pounds per second per foot of sediment dropping out of suspension. Assuming the fluidized alluvial sands have a bulk density on the order of 80 pounds per cubic foot, this results in about 1 cubic yard per lineal foot of deposition upstream of the structure every 8 to 10 seconds. Flood flows diverted around the structure can be equally as damaging, now confined to the sidewalls of the structure, with an increased unit discharge and increased scour potential adjacent the structure.

The preceding example illustrates the value of designing elevated structures that are at risk from flood scour, with the entire structure founded on a series of drilled piers designed in conformance with the applicable requirement outlined in Section 2 of the Borrego Valley Flood Management Report. Specifically, structures should be designed so that the entire design flow can pass between obstructions and exit at the downstream end of the property in its natural condition, without negative effects on the neighboring property. Thus, regardless of the actual regime conditions, a residential development can be built on the upper flanks of an alluvial fan and properly designed to minimize the risk from flood scour by minimizing any impediments to non-constrained flood flows down the face of the alluvial fan.

Given the preceding table for the Borrego Palm Canyon structure, which summarizes the hydraulic conditions for the three regime models, with corresponding flow velocities ranging from 9.8 to almost 17 feet per second, a more detailed scour study was also conducted using the Federal Highway Administration Hydraulic Engineering Circular No. 18 (HEC-18). A summary of the hydraulic design conditions specific to the site are listed below using the County's methodology, along with the three regime models. Engineering calculations for the HEC-18 evaluation are also included in Appendix A and summarized in the following paragraphs.

	County Method	Regime Models		
		Dawdy	Cabazon	Rams Hill
Q100 (cfs)	11,700	11,700	11,700	11,700
Flow Depth (ft)	2 - 2¼	2.97	2.28	0.98
Regime Width (ft)	---	402.7	274.2	1,129.8
Velocity (fps)	6½ - 7	9.70	18.54	10.61
Froude No.	1	1	2.17	1.89
Manning's n value	---	0.057	0.025	0.025

NOTES: - $S = 0.033$ through the study area
 - $n = 0.025$ except for the Dawdy method, which assumes critical flow conditions
 - The County method values were interpreted from the Flood Hazard Map contained in the 1989 Borrego Valley Flood Management Report. The range in values results for flood flows originating from the Hellhole/Fire Canyon or the Borrego Palm Canyon.

Note also that with the Cabazon model, the computed velocity of over 18 feet per second seems unreasonably high and the regime width unreasonably low. Discounting these criticisms, and as indicated in the following paragraphs and the supporting calculations, scour depth is a function of upstream flow depth and Froude number, with the Cabazon method actually generating very similar scour depths to those calculated by the Dawdy method.

Note that both the County method and the Dawdy method are based on the critical depth assumption, which is inappropriate when conducting a more rigorous scour analysis. For this scour analysis, we have used the site-specific channel bed slope of 0.033. For these conditions, a supercritical flow regime exists when using both the Rams Hill and Cabazon models, with Froude Nos. of 1.89 and 2.17, with corresponding flow velocities of 10.61 and 18.52 for the Rams Hill and Cabazon models, respectively. Because of their wide variances in regime widths, the

supercritical flow depth for the Rams Hill model is 0.98 foot, while the Cabazon model results in a supercritical flow depth of 2.28.

7 PIER SCOUR

The County's Borrego Valley Flood Management Report provides general design criteria for pier scour, the salient points of which are included in the supporting calculations in Appendix A. For our evaluation of pier scour, we have also used the Federal Highway Administration's November 1995 Hydraulic Engineering Circular No. 18 - Evaluating Scour Bridges, Third Edition, Publication No. FHWA-IP-90-017 (HEC-18), along with Melville and Coleman's (2000) Bridge Scour Water Resources Publications (WRP).

HEC-18 first requires an assessment of the long-term bed elevation change, which, absent any urbanization upgradient of the project, along with the geomorphology of alluvial fans, it is safe to say that over the next 100 years, there should be no significant long-term trend in either aggradation or degradation of the alluvial fan surface. While HEC-18 goes on to describe a variety of scour mechanisms, the only one of practical relevance to the subject project is the local scour that occurs at piers resulting from the stagnation pressure of impinging flood flows on the upstream side of the pier.

In our analyses, we have assumed that the drilled pier would be reinforced with steel I-beams, specifically an M 4X13 encased in a 12-inch-diameter concrete shaft. Conventional steel reinforcing could also be used.

The CSU equation has been used to evaluate local pier scour as described in HEC-18. Figure 6, below, from HEC-18 provides a graphical representation of scour depth as a function of pier width.

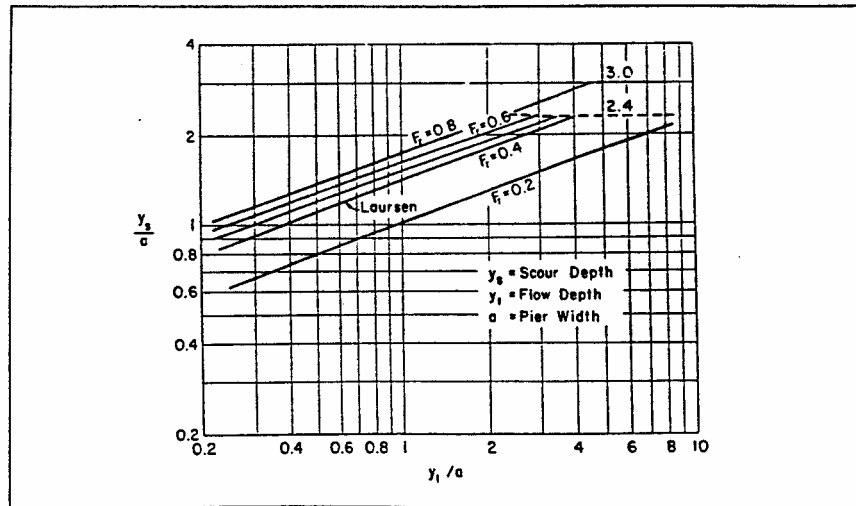


Figure 6. Values of y_s/a vs. y_1/a for CSU's equation.⁽⁴⁷⁾

Fig. 6, HEC-18

This relationship can be expressed mathematically as follows:

$$\frac{y_s}{y_1} = 2.0 K_1 K_2 K_3 K_4 \left(\frac{a}{y_1} \right)^{0.65} Fr_1^{0.43} \quad (\text{Eq. 21, HEC-18})$$

where:

- y_s = Scour depth, ft
- y_1 = Flow depth directly upstream of the pier, ft
- K_1 = Correction factor for pier nose shape from Figure 7 and Table 2 = 1
- K_2 = Correction factor for angle of attack of flow from Table 3 or Equation 23 = 1
- K_3 = Correction factor for bed condition from Table 4 = 1.1
- K_4 = Correction factor for armoring by bed material size from Equation 24 and Table 5 = 1
- a = Pier width, ft = 1 ft
- Fr_1 = Froude Number directly upstream of the pier = $V_1/(gy_1)^{1/2}$

Rams Hill Model w/1-foot-diameter Piers

$$\frac{y_s}{y_1} = 2.0 * 1 * 1 * 1.1 * 1 * \left(\frac{1}{0.98} \right)^{0.65} * 1.89^{0.43} = 2.93$$

or

$$y_s = 2.87 \text{ ft}$$

Please note that K_4 decreases scour depths for armoring of the scour hole for bed materials that have a $d_{50} \geq 60$ mm. As the d_{50} of the alluvial sands is on the order of 1.0 mm, the value of K_4 is 1.0.

7.1 Scour from Debris on Piers

Debris production within the semi-arid ephemeral systems of the Pacific Southwest is at times significant and the likelihood for debris accumulation on structure foundations must be considered in design, as it increases both scour and lateral loading from the larger frontal area provided by the debris raft. Appendix G of HEC-18 provides an interim procedure for estimating the effect of debris on local scour at piers. However, as stated in the appendix, "Engineering judgment and experience is used to determine the width, w [of the debris raft]." As no design guidelines are provided for selection of a reasonable debris raft size, we have elected to use design criteria developed by Melville and Dongol (1992), as described in the WRP document and referenced in HEC-18. The discussion on debris loading contained in the WRP has been reproduced and is included in Appendix B for completeness. McClellan (1994), as part of his work on the subject, concluded that under low Froude Number conditions, the debris rafts tended to be shallow and extensive in plan area, while under high Froude Number conditions, the debris rafts tended to be deep and narrow. The WRP data suggested floating debris raft thicknesses varying from 0.52 to 1.64 times the pier diameter, and the floating debris raft diameter varying from 2.1 to 6.9 times the pier diameter. Moreover, the maximum local scour depth recorded in model studies was $3.6 * b$ [α when using the HEC-18 nomenclature; "b" is used here as it is referenced in Appendix B], representing a 50 percent increase over that of a uniform circular pier ($d_s = 2.4*b$). Given this criteria, and assuming a Froude Number on the order of 2 to be considered high, we have assumed the following:

$$b_d \cdot 2.5 \cdot \text{diameter}$$

$$T_d \cdot 1.5 \cdot \text{diameter}$$

The equivalent debris raft pier diameter for the Rams Hill model with a 12-inch-diameter drilled pier is then calculated as follows:

$$b_e = \frac{0.52T_d b_d + (y - 0.52T_d)b}{y} \quad (\text{Eq. 6.22, WRP})$$

$$b_e = \frac{0.52 * 1.5 * 2.5 + (0.98 - 0.52 * 1.5) * 1}{0.98}$$

$$b_e = 2.19 \text{ feet}$$

Inserting this equivalent pier diameter into Eq. 21, HEC-18, then yields the effects of a debris raft on local scour fronting a 12-inch drilled pier, as follows:

$$\frac{y_s}{y_1} = 2.0 * 1 * 1 * 1.1 * 1 * \left(\frac{2.19}{0.98} \right)^{0.65} * 1.89^{0.43} = 4.88$$

or

$$y_s = 4.78 \text{ ft}$$

7.2 Width of Scour Holes

The top width of the scour hole has been approximated as $2.0 y_s$, as suggested in Figure 13 (HEC-18) and reproduced below.

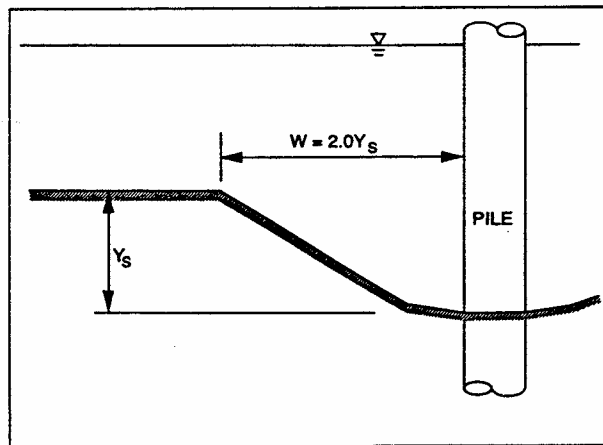


Figure 13. Topwidth of scour hole.

Fig. 13, HEC-18

This suggests scour holes around 12-inch-diameter drilled piers may approach 10 feet in their top width.

As indicated in both HEC-18 and WRP, the design scour depth includes both general scour and local scour, the latter of which results from any variety of obstructions within the floodway. For this project, local scour is limited only to pier scour, which is described in the previous paragraphs as a function of the upstream water depth, the Froude No., and the structure characteristics. The County also provides design criteria for pier scour as a function of velocity and pier diameter.

General scour, or simply the variation in bed form, is also usually expressed in terms of upstream water depth, with recommended ranges in general scour varying from 1 to 2 times the upstream water depth. The WRP recommends $1\frac{1}{2} y_1$; the County's method describes general scour on the face of an alluvial fan as a function of velocity and, for 6 to 8 feet per second, recommends, $1.8 y_1$. HEC-18 recommends general scour depths in braided streams ranging from 1 to 2 times the upstream water depth. In our analysis, we have used a general scour depth of $1.5 y_1$ and also carried forward, in its entirety, the County method for comparison with the design scour depths determined from the various regime model methods. The following table

summarizes the design water depth using both the HEC-18 approach for the various regime models, along with the County method.

Design Scour Parameters

Regime Model	y_1	V	F_r	y_s	y_s^*	\bar{y}	y_{total}
Dawdy	2.97	9.70	1	3.22	3.99	4.46	8.45
Cabazon	2.28	18.54	2.17	4.10	5.35	3.42	8.77
Rams Hill	0.98	10.61	1.89	2.87	4.78	1.47	6.25
County	2 - 2¼	6½ - 7	1	3.5	3.5	1.8 - 2.03	5.3 - 5.53

NOTES: As indicated previously, the range in County values represents flood flows out of the Hellhole/Fire Canyon and the Borrego Palm Canyon alluvial washes.

- y_s represents the local scour associated with the pier obstruction
- y_s^* represents the local scour associated with a debris rack accumulating around the pier
- The design scour depth, y_{total} , is the summation of both general scour, y and y_s^* .

As indicated in the preceding table, the HEC-18 design scour depth is similar to the County's design scour depth regardless of the regime model. However, when the debris rack is included in the local scour evaluation, all regime models then estimate larger scour depths than the County method. For these conditions, the debris rack around a 12-inch-diameter drilled pier is estimated to have a width of 2.5 feet and a depth of 1.5 feet, resulting in an effective equivalent pier diameter ranging from 1.39 to 2.19, depending upon the regime model selected (see Page 12 of the calculations), which results in local pier scour associated with debris loading ranging from 4.0 to 5.4 feet.

Given the preceding discussions regarding inconsistencies in the Dawdy model and the unreasonably high velocities and narrow regime widths in the Cabazon model, we have used the Rams Hill regime model for estimating the design scour depth, including the debris rack, which results in a design scour depth of 6.25 feet compared to the County's 5.3 to 5.53 foot design scour depth.

Given the design scour depth, the structure must then be elevated above the 100-year design flood level, which the County specifies as 2 to 2¼ feet for design storms originating out of the Hellhole/Fire Canyon and Borrego Palm Canyon alluvial fans, respectively. Accordingly, we recommend a minimum 3-foot clear space above the highest adjacent topography as the bottom cord elevation of the structural first floor of any elevated structures.

For at-grade structures, including access drives, not influenced by the presence of drilled piers, the design general scour depth, depending upon the selected model, ranges from about 1.5 to 4.5 feet and, given the previous considerations, we would recommend a minimum cut-off wall depth of 3 feet.

It should be noted that driveway or concrete slabs adjacent to drilled piers can become undermined by the localized scour hole developing around the pier, with a maximum surface expression of approximately two times the pier scour depth. Accordingly, we recommend that the surface expression of any pier scour hole be estimated to have a radius of 10 feet measured from the centerline of the drilled pier and surface improvements designed to accommodate these local scour holes.

8 FOUNDATION DESIGN RECOMMENDATIONS

8.1 Lateral Pier Capacity

In keeping with the County's requirements in the 1989 Borrego Valley Flood Management Report, the entire residential structure should be founded on a series of drilled piers, with the bottom elevation of the structural floor joists a minimum of 3 feet above the highest adjacent grade. As indicated previously, we have assumed that all piers will be 12-inch diameter cast in drilled hole shafts, reinforced with a steel wide flange, M 4X13, with its strong axis pointing upgradient. Piers shall be designed to accommodate a total cantilevered height of 9¼ feet when exposed to flood waters loading both the debris rack and the remaining exposed concrete shaft. For this condition, the design lateral load applied to each drilled pier is 1,255 pounds with a corresponding induced moment of 6,755 foot-pounds. As the design wind or

seismic loads will not occur during a 100-year design storm, we suggest that the design unsupported drilled pier height for resisting seismic or wind loads be on the order of 3 to 4 feet, assuming some level of wind loading could accompany some level of flood-induced scour adjacent to drilled pier foundations. In our analyses, we have assumed a 4-foot cantilevered pier height for wind and seismic loads.

Resistance to lateral loads applied to drilled piers is developed through deflection in the pier, which mobilizes the reaction of the soil into which the pier is embedded. The resisting pressure applied by the soil to the pier depends upon the relative stiffness of the pier and soil, as well as the depth of embedment.

Failure of a laterally-loaded pier takes place either when the maximum bending moment in the loaded pier reaches the ultimate or yield resistance of the pier section, or when the lateral earth pressures reach the ultimate lateral resistance of the soil along the total length of the pier. For purposes of definition, failure of piers with relatively "short embedment" takes place when the pier rotates as a unit with respect to a point located close to its toe. Failures of piers with relatively "long embedment" occur when the maximum bending moment applied to the pier exceeds the yield resistance of the pier section, and a plastic hinge forms at the section of maximum bending moment. Investigators have suggested that piers be grouped relative to their dimensionless depth of embedment, L/T , where:

$$L = \text{embedment length of the pier in feet, and}$$
$$T = \left(\frac{EI}{f} \right)^{\frac{1}{5}} \text{ (divided by 12 to convert inches to feet)}$$

Short piers are generally defined as L/T being less than 2.0, and long piers are generally defined as L/T being larger than 4.0.

The quantity EI is the stiffness of the drilled pier, and f (coefficient of variation of soil modulus) would be on the order of 40 pounds per cubic inch for the alluvial sands.

The structural capacity and load deformation characteristics of the drilled piers can then be determined using the elastic theory approach developed by Matlock and

Reese (1962). A condensed version of this approach is outlined in the NAVFAC Design Manual DM-7.02, Chapter 5, Section 7, a copy of which is included in Appendix C. Calculations are also provided in Appendix A demonstrating the capacity for the 100-year design flood debris rack loading, along with a maximum suggested allowable lateral capacity for seismic/wind loading of 1,650 pounds per drilled pier.

8.2 Axial Pier Capacity

Axial pier capacity is based on an assumed minimum design embedment depth of $12\frac{3}{4}$ feet (22 feet total) to accommodate the design lateral capacity, and an allowable soil adhesion value of 600 pounds per square foot applied below the design scour depth. For this condition, a 12-inch-diameter cast-in-drilled-hole pier embedded into the medium dense to dense alluvial deposits would have an allowable axial capacity of 24,700 pounds per pier. If any additional axial capacity is needed, pier depths can be deepened accordingly.

8.3 Alternative Foundation Types

Although this report focuses on drilled pier foundations, alternate foundation types can be used when consistent with the design criteria contained in the County's Borrego Valley Flood Management Report and when supported by an "engineering study", as described on Pages 21 and 22 of Appendix II of the Borrego Valley Flood Management Report.

REFERENCES

- Ackers, P., and White, W.R., Sediment Transport: New Approach and Analysis, in Journal of the Hydraulics Division, Proceedings of the American Society of civil Engineers, Vol. 99, No. HY11, Nov. 1973, pp. 2041 - 2060.
- Boyle Engineering Corporation, October 1989, Borrego Valley Flood Management Report.
- Chang, Howard H., "Fluvial Processes in River Engineering," John Wiley & Sons, New York, 1988.
- Dawdy, David R., 1979, Flood Frequency Estimates on Alluvial Fans, in Journal of the Hydraulics Division, Proceedings of the American Society of Civil Engineers, Vol. 105, No. HY11, Nov. 1979, pp.1047 © 1413.
- Dawdy, David R., "Flood Frequency Estimates on Alluvial Fans," Closure in Journal of the Hydraulics Division, Proceedings of the American Society of Civil Engineers, Vol. 107, No. HY3, March 1981, pp. 379 and 380.
- Denny, Charles S., "Alluvial Fans in the Death Valley Region, California and Nevada," Geological Survey Professional Paper 466, 1965.
- Engelund, F., and Hansen, E., "A Monograph on Sediment Transport in Alluvial Streams," Teknisk Vorlag, Copenhagen, Denmark, 1967.
- Federal Emergency Management Agency, February 1989, FEMA Report No. 165, Alluvial Fans: Hazards and Management.
- Federal Highway Administration, November 1995, Evaluating Scour at Bridges, 3rd Edition, Hydraulic Engineering Circular No. 18, Publication No. FHWA-IP-90-017.
- French, Richard H., "Flood Hazard Assessment on Alluvial Fans: An Examination of the Methodology," prepared for the U.S. Department of Energy, Nevada Operations Office, Publication No. 45040, August 1984.
- Gerrard, John, "Alluvial Soils," Van Nostrand Reinhold Company, New York, 1987.

REFERENCES (continued)

- Graf, Walter H., "Hydraulics of Sediment Transport," McGraw-Hill Book Company, New York, 1971.
- Group Delta Consultants, October 1989, Borrego Valley Flood Management Report, Appendix III, Technical Basis for Design and Structural Improvements.
- Group Delta Consultants, Crampton, W.F., 1988, Sewage Disposal Feasibility Study, Montezuma Valley Road Property, Borrego Springs, California, APN 197-031-03, APN 197-040-38, APN 198-010-19.
- Guy, H.P, Simons, D.B., and Richardson, E.V., "Summary of Alluvial Channel Data from Flume Experiments, 1956-61," Geological Survey Professional Paper 462-1, 1966.
- Leopold, Luna B., and Maddock, T., 1953, The Hydraulic Geometry of Stream Channels and Some Physiographic Implications, Geological Survey Professional Paper 252.
- Leopold, Luna B., and Miller, John P., Ephemeral Streams Hydraulic Factors and Their Relationship to the Drainage Net," Geological Survey Professional Paper 282-A, 1956.
- Leopold, Luna B., and Wolman, Gordon M., "River Channel Patterns: Braided, Meandering and Straight," Geological Survey Professional Paper 282-B, 1957.
- McClellan, A.K., 1994, "Process of Debris Accumulation on Bridge Piers," M. Eng. thesis, University of Louisville, Louisville, Kentucky, 74 pp.
- McGinn, R.A., "Flood Frequency Estimates on Alluvial Fans," Discussion in Journal of the Hydraulics Division, Proceedings of the American Society of civil Engineers, Vol. 106, No. HY10, Oct. 1980, pp. 1718 - 1720.
- Melville and Coleman, 2000, Bridge Scour, Water Resources Publications.
- Melville, B.W., and Dongol, D.M.S., 1992, Bridge Scour with Debris Accumulation, in Journal of Hydraulic Engineering, ASCE, 118(9), 1306-1310.

REFERENCES (continued)

Nilson, Tor H., "Modern and Ancient Alluvial Fan Deposits," Van Nostrand Reinhold Company, New York, 1985.

PRC Toups, J. Thielmann, June 1980, Cabazon Flood Study.

Reineck, H.E., and Singh, I.B., "Depositional Sedimentary Environments," Springer-Verlag, New York, 1986.

San Diego, County of, Department of Sanitation and Flood Control, "San Diego County Flood District, Zone 5, Borrego Valley, General Plan for Flood Control Improvements," July 1972.

Schumm, S.A., Mosley, M.P., and Weaver, W.E., "Experimental Fluvial Geomorphology," John Wiley & Sons, New York, 1987.

U.S. Department of the Navy, Naval Facilities Engineering Command, 1986, Foundations and Earth Structures, NAVFAC DM 7.02.

Vanoni, Vito A., Ed., 1977. Sedimentation Engineering, ASCE Manual 54, American Society of Civil Engineers, New York, 1977.

Wolman, M. Gordon, and Lucien, M. Brush, "Factors Controlling the Size and Shape of Stream Channels in Coarse Noncohesive Sands," Geological Survey Professional Paper 282-G, 1961.

Woodward-Clyde Consultants (authored by Walter F. Crampton), March 23, 1982, Design Memorandum, Geotechnical and Civil Engineering Design Services for Flood Control Facilities, Rams Hill Country Club, Borrego Springs, California.

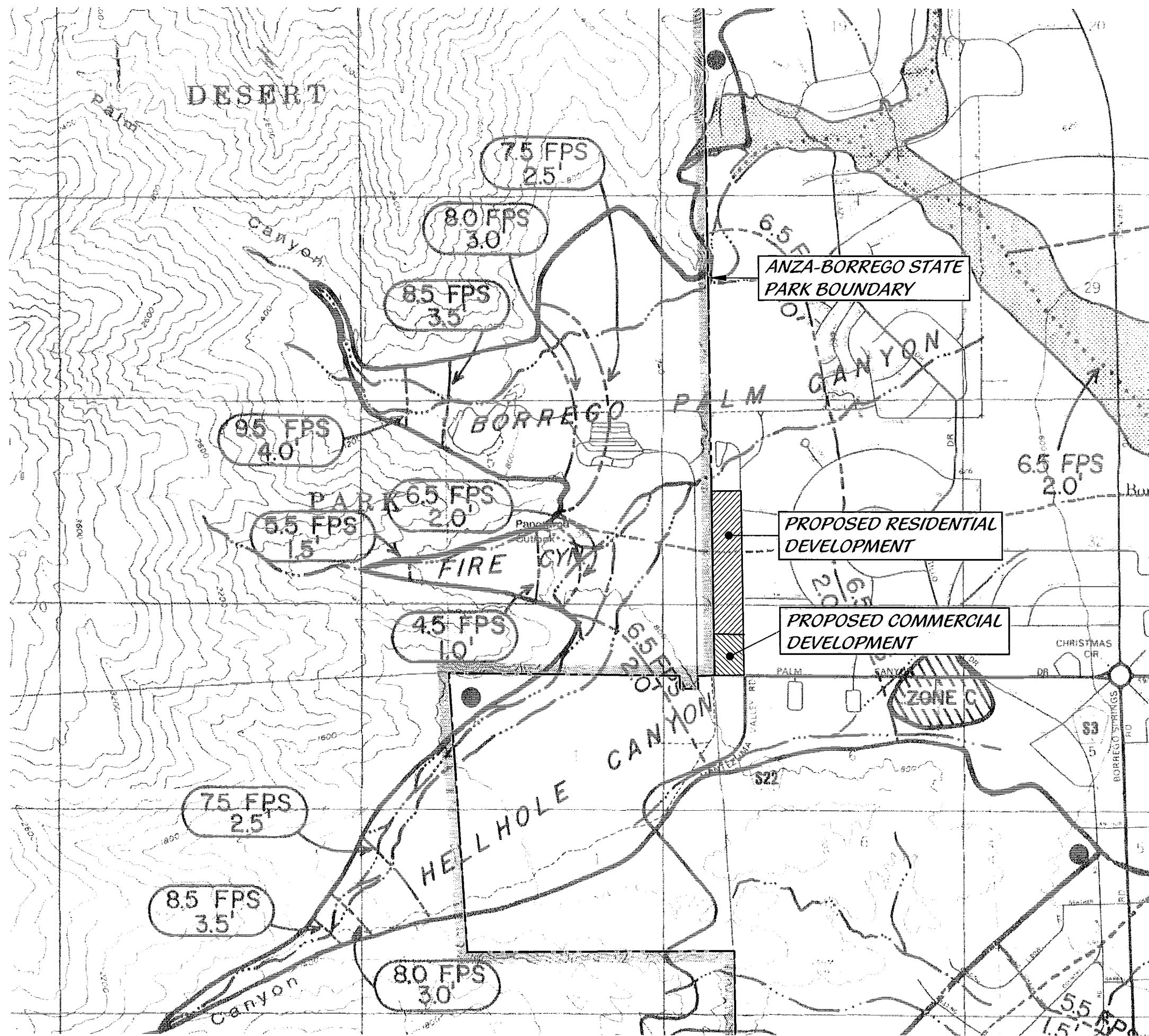
Woodward-Clyde Consultants (authored by Walter F. Crampton), October 13, 1982, Drainage and Sedimentation Study for the Proposed Rams Hill Flood Control Facility, Ram's Hill Country Club, Borrego Springs, California.


TABLE 1
REGIME CHARACTERISTICS OF STREAM CHANNELS

Station	Applicable Range in Discharge (cfs)	Measured Width (feet)	Φ	α
Cheyenne River near Hot Springs, S. Dak.	250 to 500	107 to 150	6.7	0.50
Middle Loup River at St. Paul, Nebr.	250 to 2,000	192 to 384	33.6	0.32
Rio Grande at San Acacia, N. Mex.	250 to 500	94 to 140	3.6	0.59
Rio Grande at San Felipe, N. Mex.	250 to 2,000	175 to 273	51.7	0.22
Middle Loup River at Arcadia, Nebr.	250 to 2,000	181 to 217	84.0	0.13
Smoky Hill River near Ellis, Kans.	250 to 500	115 to 148	15.8	0.36
Powder River at Arvada, Wyo.	500 to 2,000	116 to 135	62.7	0.10
Moreau River near Faith, S. Dak.	500 to 2,000	129 to 140	67.5	0.10
White River near Aglala, S. Dak.	250 to 2,000	39 to 72	7.4	0.30
Belle Fourche River below Moorcroft, Wyo.	250 to 2,000	59 to 115	10.8	0.31
Virgin River at Virgin, Utah	250 to 2,000	92 to 160	22.1	0.26
Rio Puereo at Rio Puerco, N. Mex.	250 to 2,000	66 to 133	5.9	0.43
Rio Grande near Bernalillo, N. Mex.	1,000 to 2,000	260 to 265	211.2	0.03
Saline River near Russell, Kans.	250 to 2,000	66 to 145	8.6	0.37
Smoky Hill River at Ellsworth, Kans.	250 to 2,000	92 to 122	42.2	0.14
Republican River near Bloomington, Nebr.	250 to 500	92 to 135	5.9	0.50
Bighorn River at Kane, Wyo.	250 to 2,000	152 to 175	110.3	0.06
Bighorn River at Thermopolis, Wyo.	500 to 2,000	179 to 215	74.4	0.14
Bighorn River at Manderson, Wyo.	250 to 2,000	130 to 210	38.9	0.22
Grand River at Shadehill, S. Dak.	250 to 2,000	80 to 140	21.4	0.25


TABLE 2
REGIME RELATIONS FOR VARIOUS RIVERS

Reporter	α	δ	w	Location	Remarks
Leopold et al. (1953)	$Q^{0.26}$	$Q^{0.40}$	$Q^{0.34}$	20 river cross sections representing a large variety of rivers in the Great Plains and the Southwest of the U.S. (semiarid conditions)	Variations of hydraulic characteristics in a particular cross section
Leopold et al. (1964)	$Q^{0.04}$	$Q^{0.41}$	$Q^{0.55}$	Brandywine Creek, Pennsylvania (humid eastern U.S.)	Variation of hydraulic characteristics in a particular cross section
Leopold et al. (1964)	$Q^{0.12}$	$Q^{0.45}$	$Q^{0.43}$	Average of 158 gaging stations in the U.S.	Variation of hydraulic characteristics in a particular cross section
Leopold et al. (1953)	$Q^{0.5}$	$Q^{0.4}$	$Q^{0.1}$	20 river cross sections representing a large variety of rivers in the Great Plains and the Southwest of the U.S. (semiarid conditions)	Variation of hydraulic characteristics in a downstream direction; for mean annual discharge
Leopold et al. (1964)	$Q^{0.13}$	$Q^{0.41}$	$Q^{0.43}$	10 gaging stations in the Rhine River	Average at a station relation
Leopold et al. (1956)	$Q^{0.5}$	$Q^{0.3}$	$Q^{0.2}$	Ephemeral streams in semiarid region of New Mexico, U.S.	Variation of hydraulic characteristics in a downstream direction; for mean annual discharge
Nash (1959)	$Q^{0.53}$	$Q^{0.27}$	$Q^{0.23}$	British and U.S. data from Nixon (1959)	For bankfull discharge
Rybkin (1947)	$Q^{0.57}$	$Q^{0.22}$	$Q^{0.21}$	Rivers in the Upper Volga and Oka Basin	Mean long-term discharge
Langbein (1964)	$Q^{0.53}$	$Q^{0.37}$	$Q^{0.10}$	---	Theoretically
Blench (1957)	$Q^{0.50}$	$Q^{0.33}$	$Q^{0.17}$	---	Regime equations for canals



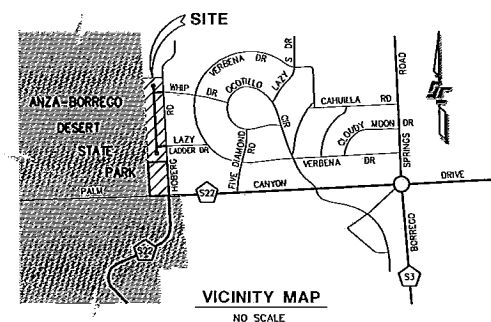
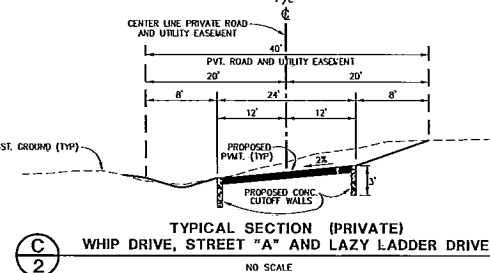
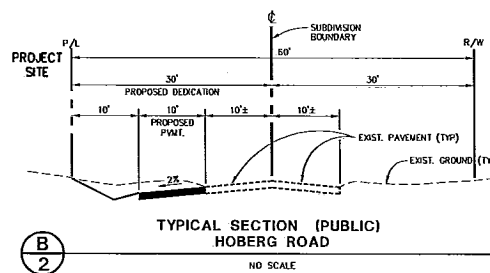
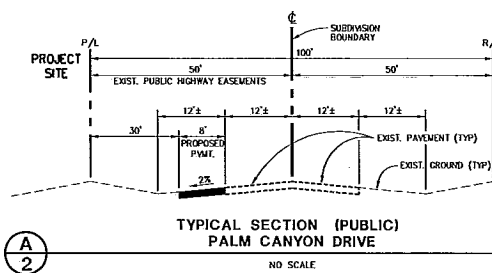
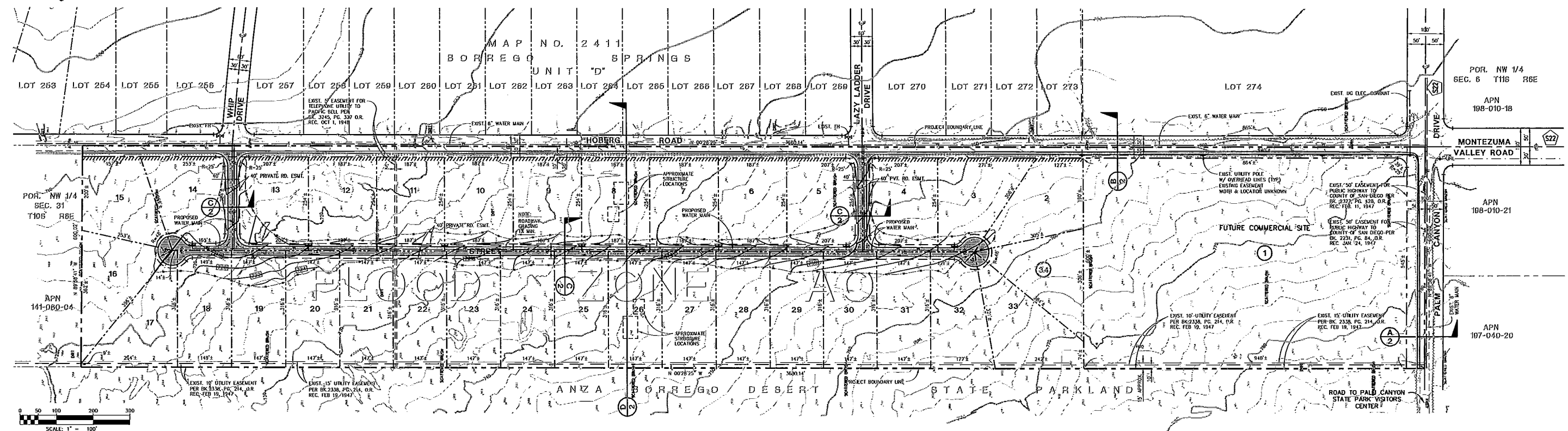

 SCALE: 1"=2000'

REPRODUCED FROM "FLOOD HAZARD MAP, BORREGO VALLEY ALLUVIAL FANS," BORREGO VALLEY FLOOD MANAGEMENT REPORT, BOYLE ENGINEERING CORP., OCTOBER 1989

	TERRACOSTA CONSULTING GROUP ENGINEERS AND GEOLOGISTS 4455 MURPHY CANYON ROAD, SUITE 100 SAN DIEGO, CA 92123 (658) 573-6900	FIGURE NUMBER 1
	PROJECT NAME BORREGO SPRINGS SUBDIVISION APN 141-080-05	PROJECT NUMBER 2418
	SITE PLAN	

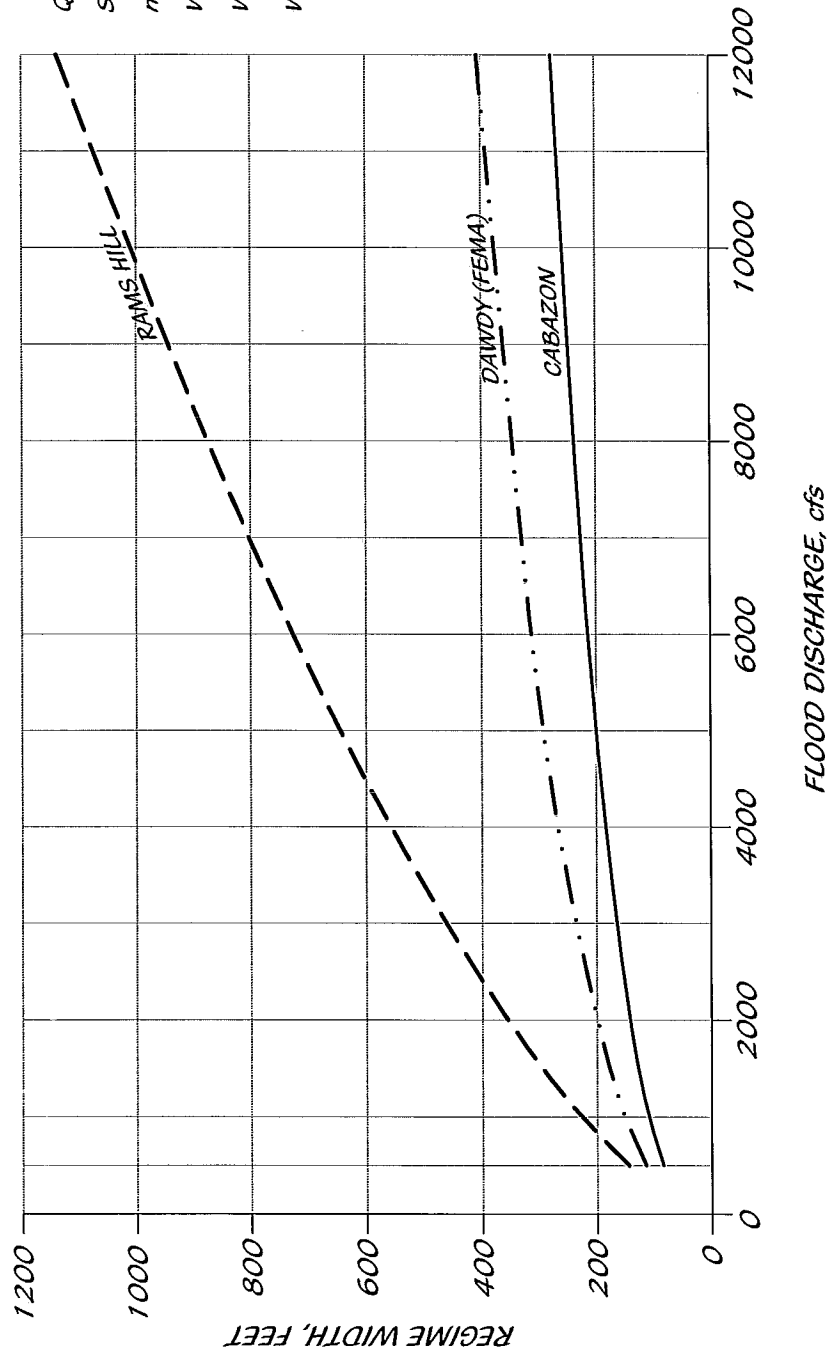
PRELIMINARY GRADING PLAN COUNTY OF SAN DIEGO TRACT

SCALE: 1" = 285'



GENERAL NOTES (PRELIMINARY GRADING)

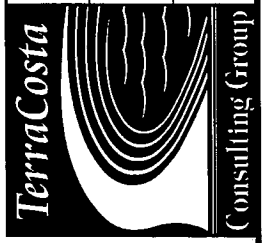
- THIS "PRELIMINARY GRADING PLAN" DOES NOT CONSTITUTE A CONSTRUCTION DOCUMENT. A FINAL GRADING PLAN, PREPARED (TO THE SATISFACTION OF THE DIRECTOR OF PUBLIC WORKS) IN ACCORDANCE WITH COUNTY GRADING ORDINANCE, SHALL BE SUBMITTED TO THE DEPARTMENT OF PUBLIC WORKS. APPROVAL OF THE FINAL GRADING PLAN SHALL BE REQUIRED AND GRADING PERMITS ISSUED PRIOR TO ANY WORK IN THE FIELD.
- A CONSTRUCTION, EXCAVATION OR ENCROACHMENT PERMIT FROM THE DIRECTOR OF PUBLIC WORKS WILL BE REQUIRED FOR ANY WORK IN THE COUNTY RIGHT-OF-WAY.
- ALL SLOPES OVER 3:1 SHALL BE PLANTED IN ACCORDANCE WITH SAN DIEGO COUNTY SPECIFICATIONS.
- A SOILS REPORT SHALL BE REQUIRED PRIOR TO THE ISSUANCE OF A GRADING AND/OR BUILDING PERMIT.
- APPROVAL OF THESE PLANS BY THE DIRECTOR OF PUBLIC WORKS DOES NOT AUTHORIZE ANY WORK OR GRADING TO BE PERFORMED UNTIL THE PROPERTY OWNER'S PERMISSION HAS BEEN OBTAINED AND A VALID GRADING PERMIT HAS BEEN ISSUED.
- THE DIRECTOR OF PUBLIC WORKS APPROVAL OF THESE PLANS DOES NOT CONSTITUTE COUNTY BUILDING OFFICIAL APPROVAL OF ANY FOUNDATIONS FOR STRUCTURES TO BE PLACED ON THE AREA COVERED BY THESE PLANS. NO WAIVER OF THE GRADING ORDINANCE REQUIREMENTS CONCERNING MINIMUM COVER OVER EXPANSIVE SOILS IS MADE OR IMPLIED (SECTIONS 87.403 & 87.410). ANY SUCH WAIVER MUST BE OBTAINED FROM THE DIRECTOR OF DPW.
- ALL SLOPES SHALL BE ROUNDED INTO EXISTING TERRAIN TO PROVIDE A CONTOURED TRANSITION FROM CUT OR FILL FACES TO NATURAL GROUND AND ADJUTING CUT OR FILL SURFACES.
- NOTWITHSTANDING THE MINIMUM STANDARDS SET FORTH IN THE GRADING ORDINANCE AND NOTWITHSTANDING THE APPROVAL OF THESE PRELIMINARY GRADING PLANS, THE PERMITTEE IS RESPONSIBLE FOR THE PREVENTION OF DAMAGE TO THE ADJACENT PROPERTY. NO PERSON SHALL EXCAVATE ON LAND SO CLOSE TO THE PROPERTY LINE AS TO ENDANGER ANY ADJACENT PUBLIC STREET, SIDEWALK, ALLEY, FUNCTION OF ANY SEWAGE DISPOSAL SYSTEM, OR ANY OTHER PUBLIC OR PRIVATE PROPERTY, WITHOUT SUPPORTING AND PROTECTING SUCH PROPERTY FROM SETTLING, CRACKING, EROSION, SLIDING, SCOUR OR OTHER DAMAGE WHICH MIGHT RESULT FROM THE GRADING DESCRIBED ON THIS PLAN. THE COUNTY WILL HOLD THE PERMITTEE RESPONSIBLE FOR CORRECTION OF NON-DEDICATED IMPROVEMENTS WHICH DAMAGE ADJACENT PROPERTY.
- ALL GRADING DETAILS WILL BE IN ACCORDANCE WITH SAN DIEGO COUNTY STANDARD DRAWINGS DS-8, DS-10, DS-11, DS-12, DS-13, DS-14, DS-15, DS-16, DS-17, DS-18, DS-19, DS-20, DS-21, DS-22, DS-23, DS-24, DS-25, DS-26, DS-27, DS-28, DS-29, DS-30, DS-31, DS-32, DS-33, DS-34, DS-35, DS-36, DS-37, DS-38, DS-39, DS-40, DS-41, DS-42, DS-43, DS-44, DS-45, DS-46, DS-47, DS-48, DS-49, DS-50, DS-51, DS-52, DS-53, DS-54, DS-55, DS-56, DS-57, DS-58, DS-59, DS-60, DS-61, DS-62, DS-63, DS-64, DS-65, DS-66, DS-67, DS-68, DS-69, DS-70, DS-71, DS-72, DS-73, DS-74, DS-75, DS-76, DS-77, DS-78, DS-79, DS-80, DS-81, DS-82, DS-83, DS-84, DS-85, DS-86, DS-87, DS-88, DS-89, DS-90, DS-91, DS-92, DS-93, DS-94, DS-95, DS-96, DS-97, DS-98, DS-99, DS-100, DS-101, DS-102, DS-103, DS-104, DS-105, DS-106, DS-107, DS-108, DS-109, DS-110, DS-111, DS-112, DS-113, DS-114, DS-115, DS-116, DS-117, DS-118, DS-119, DS-120, DS-121, DS-122, DS-123, DS-124, DS-125, DS-126, DS-127, DS-128, DS-129, DS-130, DS-131, DS-132, DS-133, DS-134, DS-135, DS-136, DS-137, DS-138, DS-139, DS-140, DS-141, DS-142, DS-143, DS-144, DS-145, DS-146, DS-147, DS-148, DS-149, DS-150, DS-151, DS-152, DS-153, DS-154, DS-155, DS-156, DS-157, DS-158, DS-159, DS-160, DS-161, DS-162, DS-163, DS-164, DS-165, DS-166, DS-167, DS-168, DS-169, DS-170, DS-171, DS-172, DS-173, DS-174, DS-175, DS-176, DS-177, DS-178, DS-179, DS-180, DS-181, DS-182, DS-183, DS-184, DS-185, DS-186, DS-187, DS-188, DS-189, DS-190, DS-191, DS-192, DS-193, DS-194, DS-195, DS-196, DS-197, DS-198, DS-199, DS-200, DS-201, DS-202, DS-203, DS-204, DS-205, DS-206, DS-207, DS-208, DS-209, DS-210, DS-211, DS-212, DS-213, DS-214, DS-215, DS-216, DS-217, DS-218, DS-219, DS-220, DS-221, DS-222, DS-223, DS-224, DS-225, DS-226, DS-227, DS-228, DS-229, DS-230, DS-231, DS-232, DS-233, DS-234, DS-235, DS-236, DS-237, DS-238, DS-239, DS-240, DS-241, DS-242, DS-243, DS-244, DS-245, DS-246, DS-247, DS-248, DS-249, DS-250, DS-251, DS-252, DS-253, DS-254, DS-255, DS-256, DS-257, DS-258, DS-259, DS-260, DS-261, DS-262, DS-263, DS-264, DS-265, DS-266, DS-267, DS-268, DS-269, DS-270, DS-271, DS-272, DS-273, DS-274, DS-275, DS-276, DS-277, DS-278, DS-279, DS-280, DS-281, DS-282, DS-283, DS-284, DS-285, DS-286, DS-287, DS-288, DS-289, DS-290, DS-291, DS-292, DS-293, DS-294, DS-295, DS-296, DS-297, DS-298, DS-299, DS-300, DS-301, DS-302, DS-303, DS-304, DS-305, DS-306, DS-307, DS-308, DS-309, DS-310, DS-311, DS-312, DS-313, DS-314, DS-315, DS-316, DS-317, DS-318, DS-319, DS-320, DS-321, DS-322, DS-323, DS-324, DS-325, DS-326, DS-327, DS-328, DS-329, DS-330, DS-331, DS-332, DS-333, DS-334, DS-335, DS-336, DS-337, DS-338, DS-339, DS-340, DS-341, DS-342, DS-343, DS-344, DS-345, DS-346, DS-347, DS-348, DS-349, DS-350, DS-351, DS-352, DS-353, DS-354, DS-355, DS-356, DS-357, DS-358, DS-359, DS-360, DS-361, DS-362, DS-363, DS-364, DS-365, DS-366, DS-367, DS-368, DS-369, DS-370, DS-371, DS-372, DS-373, DS-374, DS-375, DS-376, DS-377, DS-378, DS-379, DS-380, DS-381, DS-382, DS-383, DS-384, DS-385, DS-386, DS-387, DS-388, DS-389, DS-390, DS-391, DS-392, DS-393, DS-394, DS-395, DS-396, DS-397, DS-398, DS-399, DS-400, DS-401, DS-402, DS-403, DS-404, DS-405, DS-406, DS-407, DS-408, DS-409, DS-410, DS-411, DS-412, DS-413, DS-414, DS-415, DS-416, DS-417, DS-418, DS-419, DS-420, DS-421, DS-422, DS-423, DS-424, DS-425, DS-426, DS-427, DS-428, DS-429, DS-430, DS-431, DS-432, DS-433, DS-434, DS-435, DS-436, DS-437, DS-438, DS-439, DS-440, DS-441, DS-442, DS-443, DS-444, DS-445, DS-446, DS-447, DS-448, DS-449, DS-450, DS-451, DS-452, DS-453, DS-454, DS-455, DS-456, DS-457, DS-458, DS-459, DS-460, DS-461, DS-462, DS-463, DS-464, DS-465, DS-466, DS-467, DS-468, DS-469, DS-470, DS-471, DS-472, DS-473, DS-474, DS-475, DS-476, DS-477, DS-478, DS-479, DS-480, DS-481, DS-482, DS-483, DS-484, DS-485, DS-486, DS-487, DS-488, DS-489, DS-490, DS-491, DS-492, DS-493, DS-494, DS-495, DS-496, DS-497, DS-498, DS-499, DS-500, DS-501, DS-502, DS-503, DS-504, DS-505, DS-506, DS-507, DS-508, DS-509, DS-510, DS-511, DS-512, DS-513, DS-514, DS-515, DS-516, DS-517, DS-518, DS-519, DS-520, DS-521, DS-522, DS-523, DS-524, DS-525, DS-526, DS-527, DS-528, DS-529, DS-530, DS-531, DS-532, DS-533, DS-534, DS-535, DS-536, DS-537, DS-538, DS-539, DS-540, DS-541, DS-542, DS-543, DS-544, DS-545, DS-546, DS-547, DS-548, DS-549, DS-550, DS-551, DS-552, DS-553, DS-554, DS-555, DS-556, DS-557, DS-558, DS-559, DS-560, DS-561, DS-562, DS-563, DS-564, DS-565, DS-566, DS-567, DS-568, DS-569, DS-570, DS-571, DS-572, DS-573, DS-574, DS-575, DS-576, DS-577, DS-578, DS-579, DS-580, DS-581, DS-582, DS-583, DS-584, DS-585, DS-586, DS-587, DS-588, DS-589, DS-590, DS-591, DS-592, DS-593, DS-594, DS-595, DS-596, DS-597, DS-598, DS-599, DS-600, DS-601, DS-602, DS-603, DS-604, DS-605, DS-606, DS-607, DS-608, DS-609, DS-610, DS-611, DS-612, DS-613, DS-614, DS-615, DS-616, DS-617, DS-618, DS-619, DS-620, DS-621, DS-622, DS-623, DS-624, DS-625, DS-626, DS-627, DS-628, DS-629, DS-630, DS-631, DS-632, DS-633, DS-634, DS-635, DS-636, DS-637, DS-638, DS-639, DS-640, DS-641, DS-642, DS-643, DS-644, DS-645, DS-646, DS-647, DS-648, DS-649, DS-650, DS-651, DS-652, DS-653, DS-654, DS-655, DS-656, DS-657, DS-658, DS-659, DS-660, DS-661, DS-662, DS-663, DS-664, DS-665, DS-666, DS-667, DS-668, DS-669, DS-670, DS-671, DS-672, DS-673, DS-674, DS-675, DS-676, DS-677, DS-678, DS-679, DS-680, DS-681, DS-682, DS-683, DS-684, DS-685, DS-686, DS-687, DS-688, DS-689, DS-690, DS-691, DS-692, DS-693, DS-694, DS-695, DS-696, DS-697, DS-698, DS-699, DS-700, DS-701, DS-702, DS-703, DS-704, DS-705, DS-706, DS-707, DS-708, DS-709, DS-710, DS-711, DS-712, DS-713, DS-714, DS-715, DS-716, DS-717, DS-718, DS-719, DS-720, DS-721, DS-722, DS-723, DS-724, DS-725, DS-726, DS-727, DS-728, DS-729, DS-730, DS-731, DS-732, DS-733, DS-734, DS-735, DS-736, DS-737, DS-738, DS-739, DS-740, DS-741, DS-742, DS-743, DS-744, DS-745, DS-746, DS-747, DS-748, DS-749, DS-750, DS-751, DS-752, DS-753, DS-754, DS-755, DS-756, DS-757, DS-758, DS-759, DS-760, DS-761, DS-762, DS-763, DS-764, DS-765, DS-766, DS-767, DS-768, DS-769, DS-770, DS-771, DS-772, DS-773, DS-774, DS-775, DS-776, DS-777, DS-778, DS-779, DS-780, DS-781, DS-782, DS-783, DS-784, DS-785, DS-786, DS-787, DS-788, DS-789, DS-790, DS-791, DS-792, DS-793, DS-794, DS-795, DS-796, DS-797, DS-798, DS-799, DS-800, DS-801, DS-802, DS-803, DS-804, DS-805, DS-806, DS-807, DS-808, DS-809, DS-810, DS-811, DS-812, DS-813, DS-814, DS-815, DS-816, DS-817, DS-818, DS-819, DS-820, DS-821, DS-822, DS-823, DS-824, DS-825, DS-826, DS-827, DS-828, DS-829, DS-830, DS-831, DS-832, DS-833, DS-834, DS-835, DS-836, DS-837, DS-838, DS-839, DS-840, DS-841, DS-842, DS-843, DS-844, DS-845, DS-846, DS-847, DS-848, DS-849, DS-850, DS-851, DS-852, DS-853, DS-854, DS-855, DS-856, DS-857, DS-858, DS-859, DS-860, DS-861, DS-862, DS-863, DS-864, DS-865, DS-866, DS-867, DS-868, DS-869, DS-870, DS-871, DS-872, DS-873, DS-874, DS-875, DS-876, DS-877, DS-878, DS-879, DS-880, DS-881, DS-882, DS-883, DS-884, DS-885, DS-886, DS-887, DS-888, DS-889, DS-890, DS-891, DS-892, DS-893, DS-894, DS-895, DS-896, DS-897, DS-898, DS-899, DS-900, DS-901, DS-902, DS-903, DS-904, DS-905, DS-906, DS-907, DS-908, DS-909, DS-910, DS-911, DS-912, DS-913, DS-914, DS-915, DS-916, DS-917, DS-918, DS-919, DS-920, DS-921, DS-922, DS-923, DS-924, DS-925, DS-926, DS-927, DS-928, DS-929, DS-930, DS-931, DS-932, DS-933, DS-934, DS-935, DS-936, DS-937, DS-938, DS-939, DS-940, DS-941, DS-942, DS-943, DS-944, DS-945, DS-946, DS-947, DS-948, DS-949, DS-950, DS-951, DS-952, DS-953, DS-954, DS-955, DS-956, DS-957, DS-958, DS-959, DS-960, DS-961, DS-962, DS-963, DS-964, DS-965, DS-966, DS-967, DS-968, DS-969, DS-970, DS-971, DS-972, DS-973, DS-974, DS-975, DS-976, DS-977, DS-978, DS-979, DS-980, DS-981, DS-982, DS-983, DS-984, DS-985, DS-986, DS-987, DS-988, DS-989, DS-990, DS-991, DS-992, DS-993, DS-994, DS-995, DS-996, DS-997, DS-998, DS-999, DS-1000, DS-1001, DS-1002, DS-1003, DS-1004, DS-1005, DS-1006, DS-1007, DS-1008, DS-1009, DS-1010, DS-1011, DS-1012, DS-1013, DS-1014, DS-1015, DS-1016, DS-1017, DS-1018, DS-1019, DS-1020, DS-1021, DS-1022, DS-1023, DS-1024, DS-1025, DS-1026, DS-1027, DS-1028, DS-1029, DS-1030, DS-1031, DS-1032, DS-1033, DS-1034, DS-1035, DS-1036, DS-1037, DS-1038, DS-1039, DS-1040, DS-1041, DS-1042, DS-1043, DS-1044, DS-1045, DS-1046, DS-1047, DS-1048, DS-1049, DS-1050, DS-1051, DS-1052, DS-1053, DS-1054, DS-1055, DS-1056, DS-1057, DS-1058, DS-1059, DS-1060, DS-1061, DS-1062, DS-1063, DS-1064, DS-1065, DS-1066, DS-1067, DS-1068, DS-1069, DS-1070, DS-1071, DS-1072, DS-1073, DS-1074, DS-1075, DS-1076, DS-1077, DS-1078, DS-1079, DS-1080, DS-1081, DS-1082, DS-1083, DS-1084, DS-1085, DS-1086, DS-1087, DS-1088, DS-1089, DS-1090, DS-1091, DS-1092, DS-1093, DS-1094, DS-1095, DS-1096, DS-1097, DS-1098, DS-1099, DS-1100, DS-1101, DS-1102, DS-1103, DS-1104, DS-1105, DS-1106, DS-1107, DS-1108, DS-1109, DS-1110, DS-1111, DS-1112, DS-1113, DS-1114, DS-1115, DS-1116, DS-1117, DS-1118, DS-1119, DS-1120, DS-1121, DS-1122, DS-1123, DS-1124, DS-1125, DS-1126, DS-1127, DS-1128, DS-1129, DS-1130, DS-1131, DS-1132, DS-1133, DS-1134, DS-1135, DS-1136, DS-1137, DS-1138, DS-1139, DS-1140, DS-1141, DS-1142, DS-1143, DS-1144, DS-1145, DS-1146, DS-1147, DS-1148, DS-1149, DS-1150, DS-1151, DS-1152, DS-1153, DS-1154, DS-1155, DS-1156, DS-1157, DS-1158, DS-1159, DS-1160, DS-1161, DS-1162, DS-1163, DS-1164, DS-1165, DS-1166, DS-1167, DS-1168, DS-1169, DS-1170, DS-1171, DS-1172, DS-1173, DS-1174, DS-1175, DS-1176, DS-1177, DS-1178, DS-1179, DS-1180, DS-1181, DS-1182, DS-1183, DS-1184, DS-1185, DS-1186, DS-1187, DS-1188, DS-1189, DS-1190, DS-1191, DS-1192, DS-1193, DS-1194, DS-1195, DS-1196, DS-1197, DS-1198, DS-1199, DS-1200, DS-1201, DS-1202, DS-1203, DS-1204, DS-1205, DS-1206, DS-1207, DS-1208, DS-1209, DS-1210, DS-1211, DS-1212, DS-1213, DS-1214, DS-1215, DS-1216, DS-1217, DS-1218, DS-1219, DS-1220, DS-1221, DS-1222, DS-1223, DS-1224, DS-1225, DS-1226, DS-1227, DS-1228, DS-1229, DS-1230, DS-1231, DS-1232, DS-1233, DS-1234, DS-1235, DS-1236, DS-1237, DS-1238, DS-1239, DS-1240, DS-1241, DS-1242, DS-1243, DS-1244, DS-1245, DS-1246, DS-1247, DS-1248, DS-1249, DS-1250, DS-1251, DS-1252, DS-1253, DS-1254, DS-1255, DS-1256, DS-1257, DS-1258, DS-1259, DS-1260, DS-1261, DS-1262, DS-1263, DS-1264, DS-1265, DS-1266, DS-1267, DS-1268, DS-1269, DS-1270, DS-1271, DS-1272, DS-1273, DS-1274, DS-1275, DS-1276, DS-1277, DS-1278, DS-1279, DS-1280, DS-1281, DS-1282, DS-1283, DS-1284, DS-1285, DS-1286, DS-1287, DS-1288, DS-1289, DS-1290, DS-1291, DS-1292, DS-1293, DS-1294, DS-1295, DS-1296, DS-1297, DS-1298, DS-1299, DS-1300, DS-1301, DS-1302, DS-1303, DS-1304, DS-1305, DS-1306, DS-1307, DS-1308, DS-1309, DS-1310, DS-1311, DS-1312, DS-1313, DS-1314, DS-1315, DS-1316, DS-1317, DS-1318, DS-1319, DS-1320, DS-1321, DS-1322, DS-1323, DS-1324, DS-1325, DS-1326, DS-1327, DS-1328, DS-1329, DS-1330, DS-1331, DS-1332, DS-1333, DS-1334, DS-1335, DS-1336, DS-1337, DS-1338, DS-1339, DS-1340, DS-1341, DS-1342, DS-1343, DS-1344, DS-1345, DS-1346, DS-1347, DS-1348, DS-1349, DS-1350, DS-1351, DS-1352, DS-1353, DS-1354, DS-1355, DS-1356, DS-1357, DS-1358, DS-1359, DS-1360, DS-1361, DS-1362, DS-1363, DS-1364, DS-1365, DS-1366, DS-1367, DS-1368, DS-1369, DS-1370, DS-1371, DS-1372, DS-1373, DS-1374, DS-1375, DS-1376, DS-1377, DS-1378, DS-1379, DS-1380, DS-1381, DS-1382, DS-1383, DS-1384, DS-1385, DS-1386, DS-1387, DS-1388, DS-1389, DS-1390, DS-1391, DS-1392, DS-1393, DS-1394, DS-1395, DS-1396, DS-1397, DS-1398, DS-1399, DS-1400, DS-1401, DS-1402, DS-1403, DS-1404, DS-1405, DS-1406, DS-1407, DS-1408, DS-1409, DS-1410, DS-1411, DS-1412, DS-1413, DS-1414, DS-1415, DS-1416, DS-1417, DS-1418, DS-1419, DS-1420, DS-1421, DS-1422, DS-1423, DS-1424, DS-1425, DS-1426, DS-1427, DS-1428, DS-1429, DS-1430, DS-1431, DS-1432, DS-1433, DS-1434, DS-1435, DS-1436, DS-1437, DS-1438, DS-1439, DS-1440, DS-1441, DS-1442, DS-1443, DS-1444, DS-1445, DS-1446, DS-1447, DS-1448, DS-1449, DS-1450, DS-1451, DS-1452, DS-1453, DS-1454, DS-1455, DS-1456, DS-1457, DS-1458, DS-1459, DS-1460, DS-1461, DS-1462, DS-1463, DS-1464, DS-1465, DS-1466, DS-1467, DS-1468, DS-1469, DS-1470, DS-1471, DS-1472, DS-1473, DS-1474, DS-1475, DS-1476, DS-1477, DS-1478, DS-1479, DS-1480, DS-1481, DS-1482, DS-1483, DS-1484, DS-1485, DS-1486, DS-1487, DS-1488, DS-1489, DS-1490, DS-1491, DS-1492, DS-1493, DS-1494, DS-1495, DS-1496, DS-1497, DS-1498, DS-1499, DS-1500, DS-1501, DS-1502, DS-1503, DS-1504, DS-1505, DS-1506, DS-1507, DS-1508, DS-1509, DS-1510, DS-1511, DS-1512, DS-1513, DS-1514, DS-1515, DS-1516, DS-1517, DS-1518, DS-1519, DS-1520, DS-1521, DS-1522, DS-1523, DS-1524, DS-1525, DS-1526, DS-1527, DS-1528, DS-1529, DS-1530, DS-1531, DS-1532, DS-1533, DS-1534, DS-1535, DS-1536, DS-1537, DS-1538, DS-1539, DS-1540, DS-1541, DS-1542, DS-1543, DS-1544, DS-1545, DS-1546, DS-1547, DS-1548, DS-1549, DS-1550, DS-1551, DS-1552, DS-1553, DS-1554, DS-1555, DS-1556, DS-1557, DS-1558, DS-1559, DS-1560, DS-1561, DS-1562, DS-1563, DS-1564, DS-1565, DS-1566, DS-1567, DS-1568, DS-1569, DS-1570, DS-1571, DS-1572, DS-1573, DS-1574, DS-1575, DS-1576, DS-1577, DS-1578, DS-1579, DS-1580, DS-1581, DS-1582, DS-1583, DS-1584, DS-1585, DS-1586, DS-1587, DS-1588, DS-1589, DS-1590, DS-1591, DS-1592, DS-1593, DS-1594, DS-1595, DS-1596, DS-1597, DS-1598, DS-1599, DS-1600, DS-1601, DS-1602, DS-1603, DS-1604, DS-1605, DS-1606, DS-1607, DS-1608, DS-1609, DS-1610, DS-1611, DS-1612, DS-1613, DS-1614, DS-1615, DS-1616, DS-1617, DS-1618, DS-1619, DS-1620, DS-1621, DS-1622, DS-1623, DS-1624, DS-1625, DS-1626, DS-1627, DS-1628, DS-1629, DS-1630, DS-1631, DS-1632, DS-1633, DS-1634, DS-1635, DS-1636, DS-1637, DS-1638, DS-1639, DS-1640, DS-1641, DS-1642, DS-1643, DS-1644, DS-1645, DS-1646, DS-1647, DS-1648, DS-1649, DS-1650, DS-1651, DS-1652, DS-1653, DS-1654, DS-1655, DS-1656, DS-1657, DS-1658, DS-1659, DS-1660, DS-1661, DS-1662, DS-1663, DS-1664, DS



$Q_{100} = 11,700 \text{ cfs}$
 $S = 0.033$
 $n = 0.025$
 $W = 2.54Q^{0.65} = 1129.8' \text{ (RAMS HILL)}$
 $W = 9.5Q^{0.40} = 402.7' \text{ (DAWDY (FEMA))}$
 $W = 17.2 (Q n)^{3/8} = 274.2 \text{ (CABAZON)}$

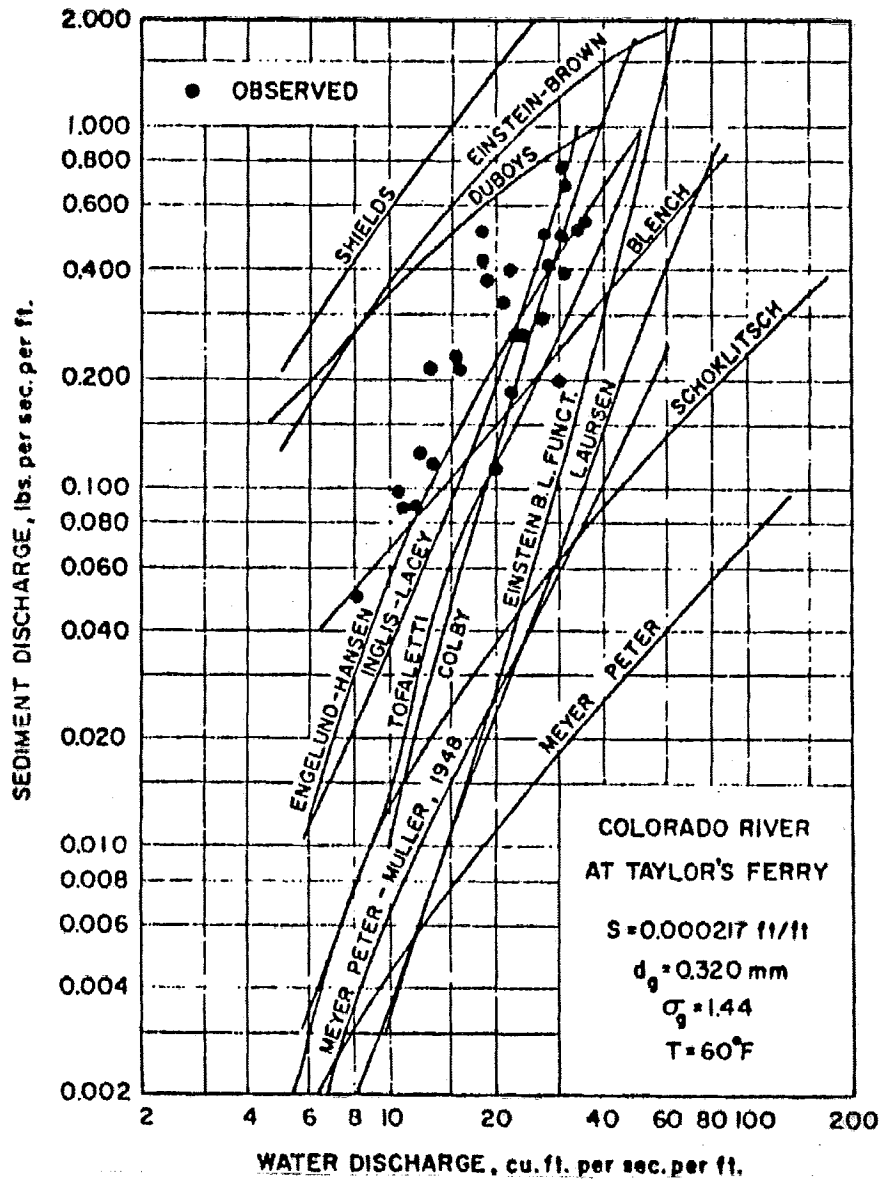
SOIL PROPERTIES

$d_{50} = 1 \text{ mm}$
 $\gamma_s = 165 \text{ pcf}$
 $V = 1.21 \times 10^{-5} \text{ ft}^2/\text{sec.}$



TERRACOSTA CONSULTING GROUP ENGINEERS AND GEOLOGISTS 4465 MURPHY CANYON ROAD, SUITE 100 SAN DIEGO, CA 92123 (858) 573-6900	PROJECT NAME BORREGO SPRINGS SUBDIVISION APN-141-080-05	FIGURE NUMBER 3 PROJECT NUMBER 2418
--	--	--

REGIME CONDITIONS



SEDIMENT DISCHARGE AS FUNCTION OF WATER DISCHARGE FOR COLORADO RIVER AT TAYLOR'S FERRY OBTAINED FROM OBSERVATIONS AND CALCULATIONS BY SEVERAL FORMULAS. REPRINTED FROM SEDIMENTATION ENGINEERING, ASCE MANUAL AND REPORT NO. 54, VANONI, ED., NEW YORK, 1975 (REPRINT 1977)



TERRACOSTA CONSULTING GROUP
ENGINEERS AND GEOLOGISTS
4455 MURPHY CANYON ROAD, SUITE 100
SAN DIEGO, CA 92123 (868) 573-6900

PROJECT NAME
BORREGO SPRINGS SUBDIVISION
APN 141-080-05

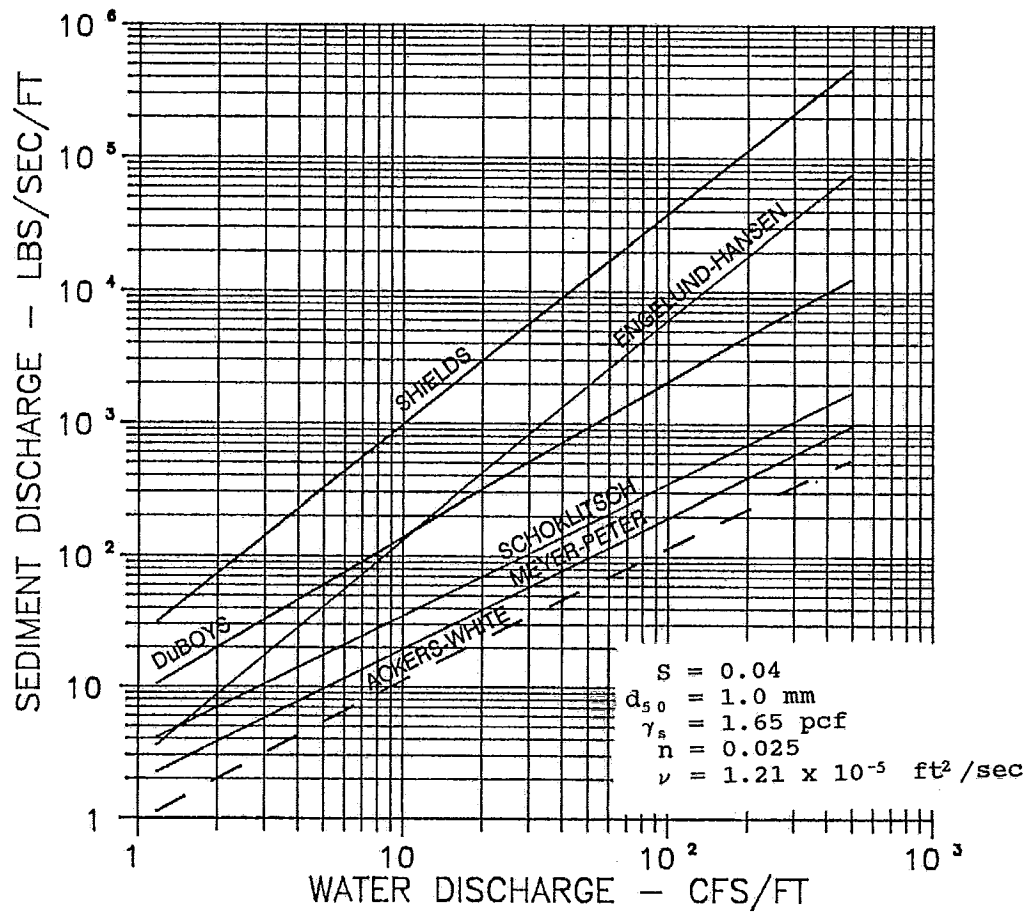
FIGURE NUMBER

4

PROJECT NUMBER

2418

SEDIMENT DISCHARGE AS
FUNCTION OF WATER DISCHARGE



SEDIMENT DISCHARGE AS A FUNCTION OF WATER DISCHARGE
COMPUTED BY SEVERAL FORMULAS



TERRACOSTA CONSULTING GROUP
ENGINEERS AND GEOLOGISTS
4455 MURPHY CANYON ROAD, SUITE 100
SAN DIEGO, CA 92123 (858) 573-6900

PROJECT NAME
BORREGO SPRINGS SUBDIVISION
APN 141-080-05

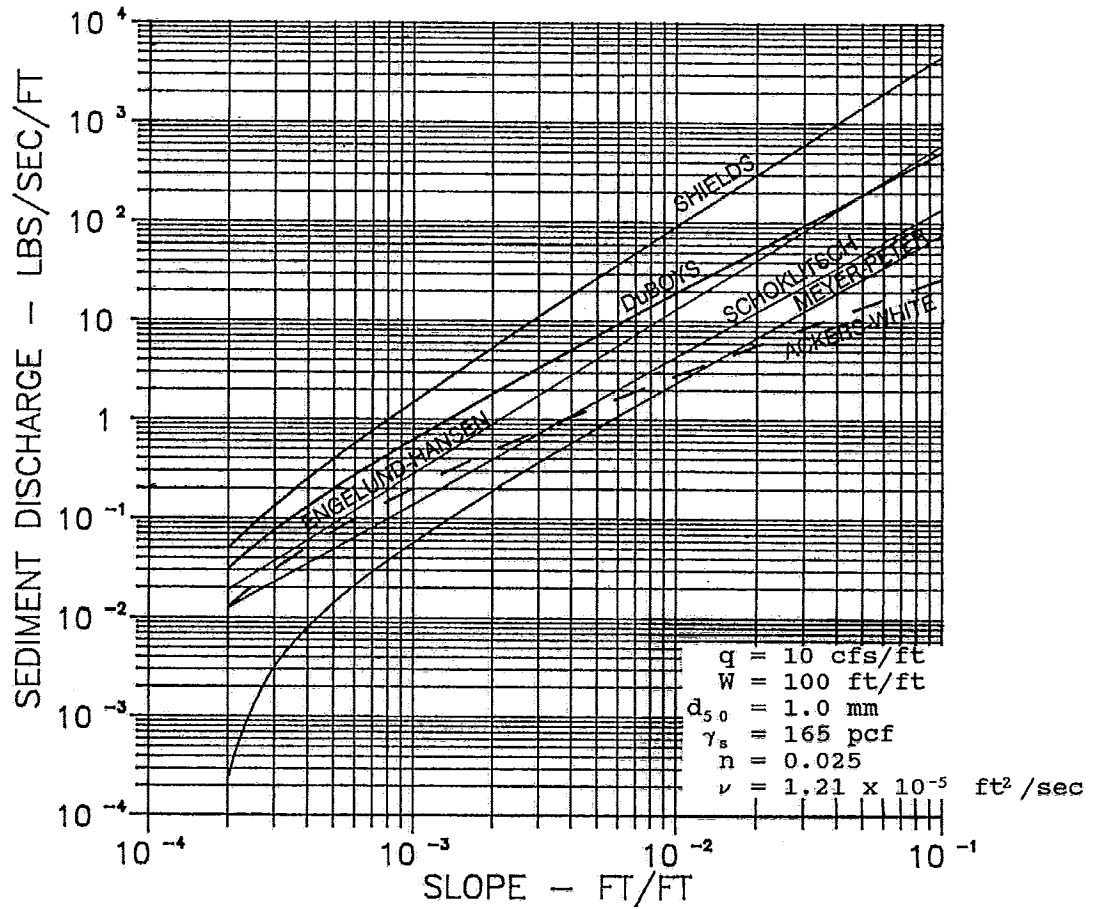
FIGURE NUMBER

5

PROJECT NUMBER

2418

SEDIMENT DISCHARGE AS A
FUNCTION OF WATER DISCHARGE



SEDIMENT DISCHARGE AS A FUNCTION OF SLOPE COMPUTED
BY SEVERAL FORMULAS



TERRACOSTA CONSULTING GROUP
ENGINEERS AND GEOLOGISTS
4455 MURPHY CANYON ROAD, SUITE 100
SAN DIEGO, CA 92123 (858) 573-8900

PROJECT NAME
BORREGO SPRINGS SUBDIVISION
APN 141-080-05

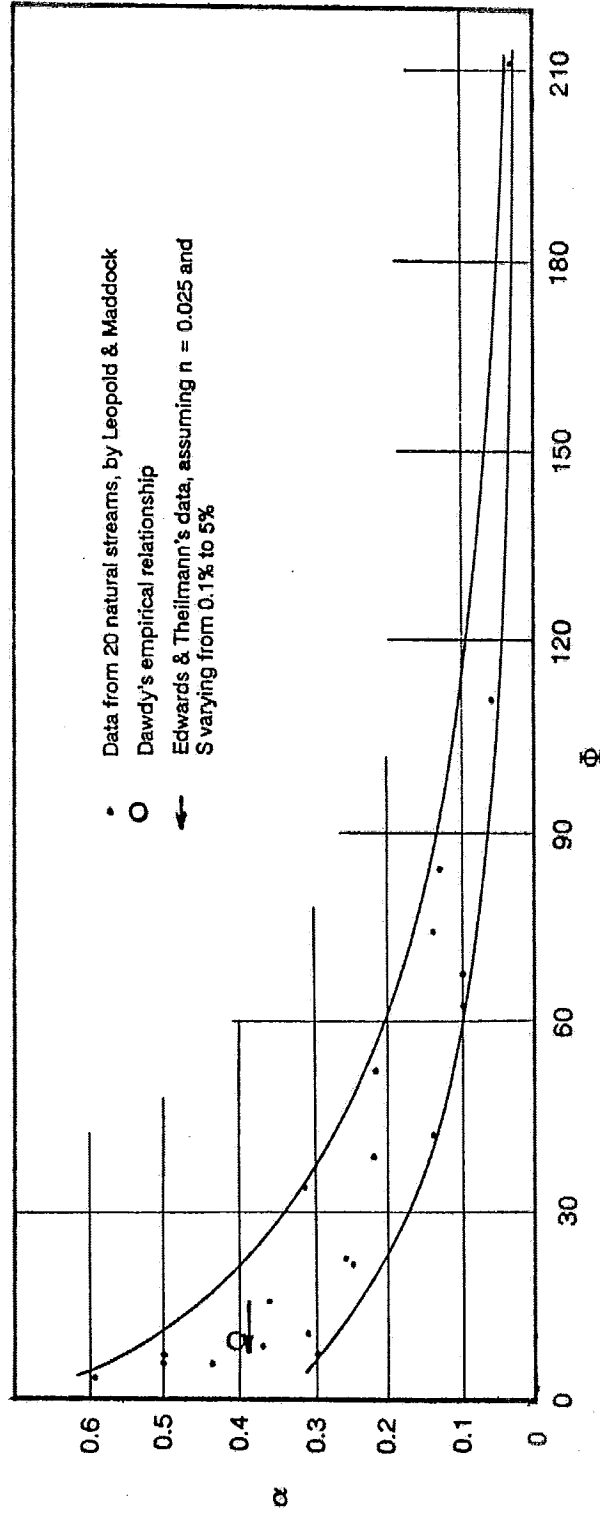
FIGURE NUMBER

6

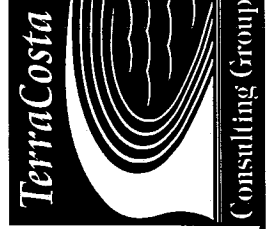
PROJECT NUMBER

2418

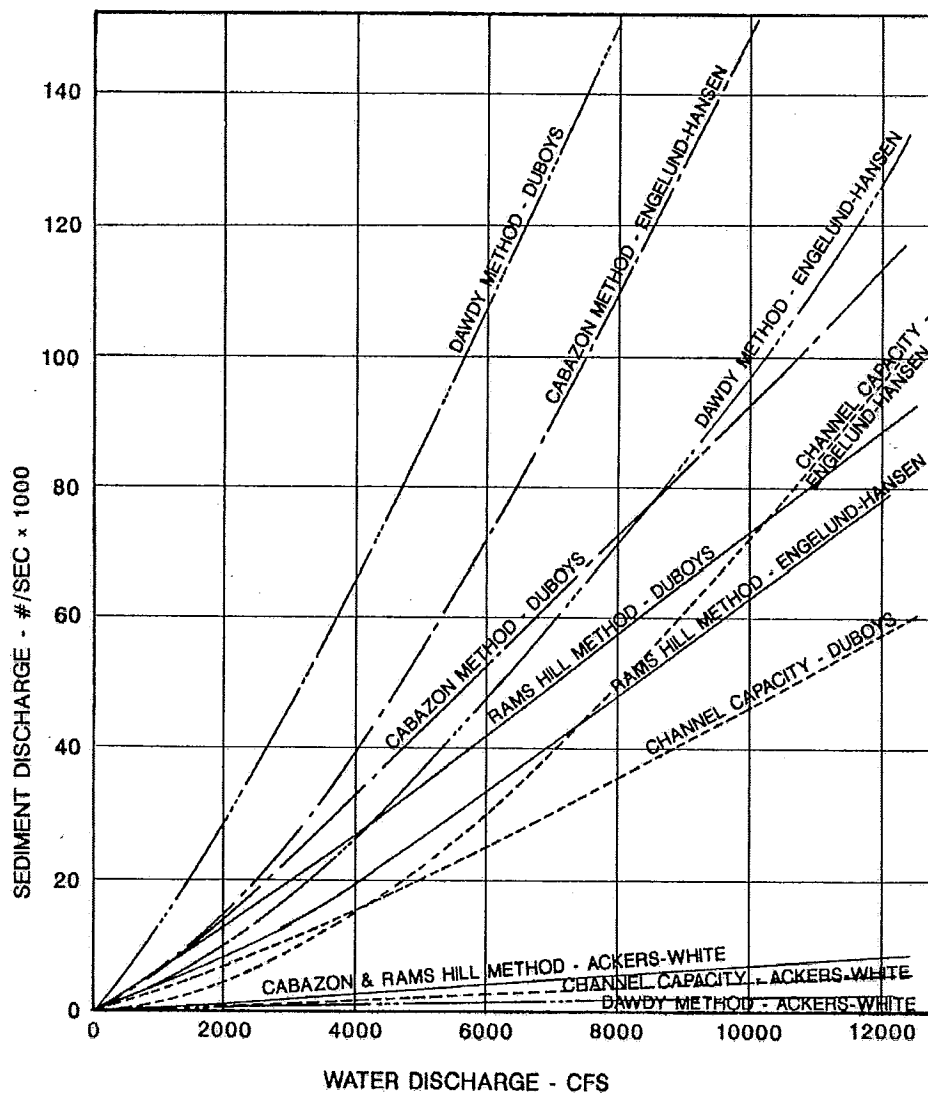
SEDIMENT DISCHARGE AS A
FUNCTION OF SLOPE



THE RELATIONSHIP OF Φ VS. α FOR 20 STREAM CHANNELS
MEASURED BY LEOPOLD & MADDOCK (1953)



TERRACOSTA CONSULTING GROUP ENGINEERS AND GEOLOGISTS 4455 MURPHY CANYON ROAD, SUITE 100 SAN DIEGO, CA 92123 (658) 573-8900	FIGURE NUMBER 7
PROJECT NAME BORREGO SPRINGS SUBDIVISION APN 141-080-05	PROJECT NUMBER 2418
THE RELATIONSHIP OF Φ VS. α	



SEDIMENT DISCHARGE CURVES FOR THE VARIOUS REGIME METHODS ALONG WITH THE SEDIMENT TRANSPORT CAPACITY FOR A 240-FOOT-WIDE CHANNEL AT A SLOPE OF 1.5%



TERRACOSTA CONSULTING GROUP
ENGINEERS AND GEOLOGISTS
4455 MURPHY CANYON ROAD, SUITE 100
SAN DIEGO, CA 92123 (858) 573-8900

PROJECT NAME
BORREGO SPRINGS SUBDIVISION
APN 141-080-05

FIGURE NUMBER

8

PROJECT NUMBER

2418

**SEDIMENT DISCHARGE CURVES
FOR VARIOUS REGIME METHODS**

APPENDIX A

CALCULATIONS

APPENDIX A
CALCULATIONS

COUNTY FLOOD PLAIN MAPS & REPORT

$$\begin{aligned}
 Q_{100} &= 11,700 \text{ cfs for BOTH BORRERO PALM & HELLHOLE / RICE} \\
 S &= 0.033 \\
 D &= 2 \text{ FT} - \text{HELLHOLE / RICE} \\
 &= 2 \frac{1}{4} \text{ FT} - \text{BORRERO PALM} \\
 V &= 6 \frac{1}{2} \text{ FPS} - \text{HELLHOLE / RICE} \\
 &= 7 \text{ FPS} - \text{BORRERO PALM}
 \end{aligned}$$

REGULATED EQUATIONS w/ $n = 0.025$

$$\begin{aligned}
 \text{RAMS HILL} - W &= 2.54 Q^{0.65} = 1128.8 \text{ FT} \\
 D &= 0.975 \text{ FT} \\
 V &= 10.61 \text{ FT/SEC} \\
 F &= 1.89
 \end{aligned}$$

NOTE: ALL HYDRAULIC CALCULATIONS CARRIED OUT AS AN ITERATIVE SOLUTION ON A HP PROGRAMABLE CALCULATOR

$$\begin{aligned}
 \text{CABERON} - W &= 17.2 (Q \text{ cfs})^{3/2} = 224.2 \text{ FT} \\
 D &= 2.283 \text{ FT} \\
 V &= 18.54 \text{ FT/SEC} \\
 F &= 2.17
 \end{aligned}$$

$$\text{DANWORTH} - W = 9.3 Q^{0.4} = 402.7 \text{ FT}$$

NOTE: THIS METHOD REQUIRES $F = 1.0$

$$F = V / \sqrt{gD} \quad \therefore V = \sqrt{gD}$$

$$Q = AV = A \sqrt{gD} = WD^{3/2} \sqrt{g}$$

$$\therefore D = \frac{Q}{W \sqrt{g}} \Bigg)^{2/3} = 2.971 \text{ FT}$$

Solving for both D & W such that $Q \approx 11,760$

$$0.0M = 0.0370$$

$$V = 9.78 \text{ FT/SEC}$$

$$F_R = 1.0$$

Plot regime widths as a function of Q

where $S = 0.033$
 $m = 0.025$

Q	Channel	Wing	Capitol
500	144.3	114.1	84.1
1000	226.4	150.6	109.0
2000	335.2	198.7	141.4
4000	557.4	262.1	183.4
8000	874.7	345.9	237.8
12000	1258.4	406.8	276.8

Plotted on
Fig. 3 of Report

PIER SCOUR

Channel method

Assume 12" ϕ drilled piers

Using Fig. II-4, Design scour = $\frac{1}{2} D_1 + D_2$

W/ $V = 6\frac{1}{2} - 7 \text{ FPS}$ $D_1 = 1.8 D = 3.6 - 4.05 \text{ FT}$

pg. 17

$D_2 = 3.5 \text{ FT}$ Assuming $\phi = 12"$

pg. 15

\therefore Design scour = $\frac{1}{2} D_1 + D_2 = 5.3 - 5.83 \text{ FT}$

Design clearance = $D + \text{Design scour}$

= $7.3 - 7.8 \text{ FT}$

TerraCosta



Consulting Group

PROJECT NAME BORRERO SPRINGS SUBDIVISION DRAWN BY W. CRAMPIN

CHECKED BY _____

PROJECT NUMBER 2418 DATE 7-12-06 PAGE 2 OF 19

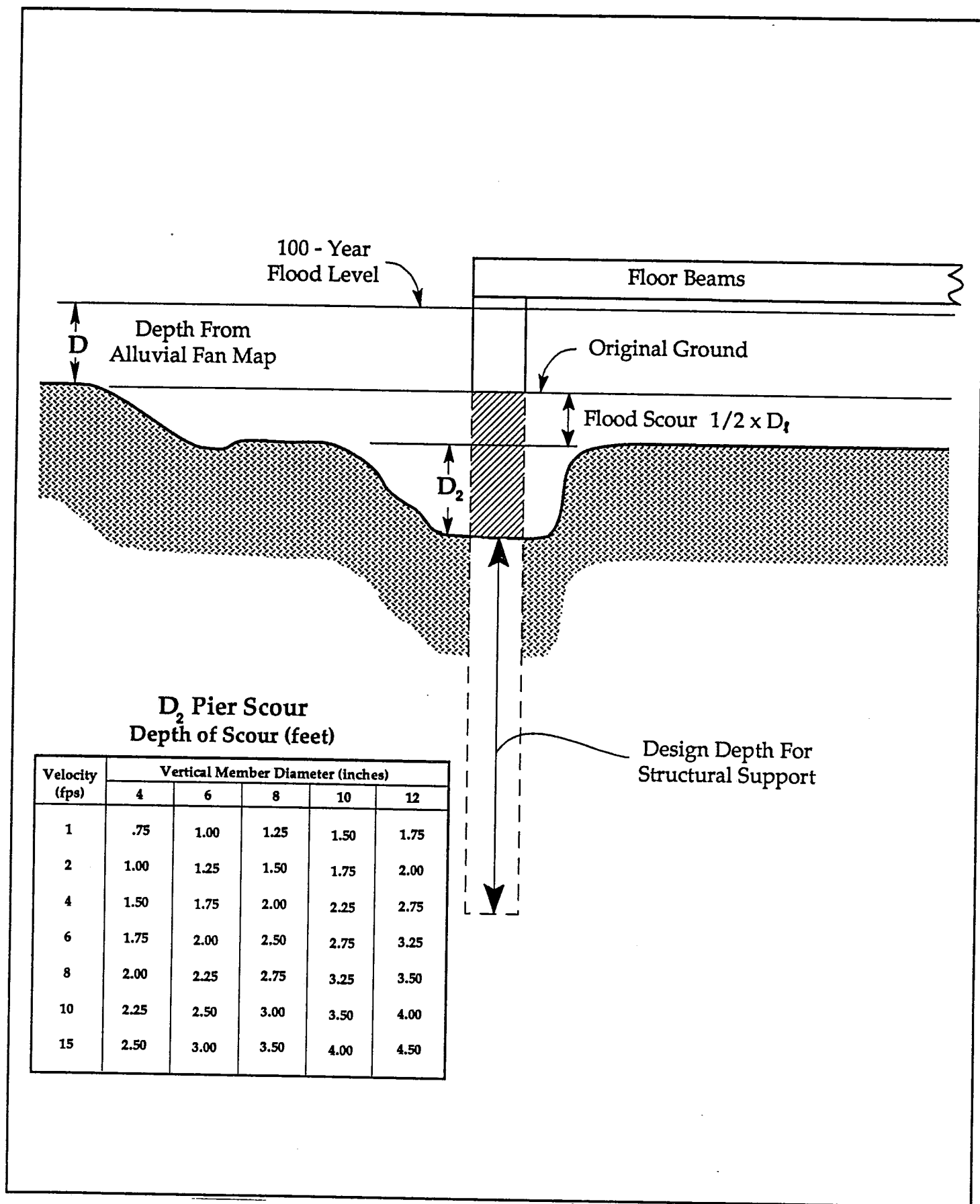


FIGURE II - 4. ADDITION OF SCOUR DEPTHS FOR PILINGS

SOURCE: BORRERO VALLEY
FLOOD MANAGEMENT
REPORT

3. Foundations

a. Structures

Structures must be constructed in such a way that foundations will be protected from erosion. Refer to Figures II-1 through II-5 for typical examples of foundation protection. Other types of protection can be used with appropriate engineering design.

The criteria given in this section are the minimum recommended for foundation protection. The variable nature of desert flooding makes determination of protection difficult.

The criteria defined may not provide protection from all future flood events. As part of any construction project, more stringent criteria for foundation protection may be used. The option of developing a more detailed flood hazard analysis is also available.

b. Depth of Erosion Protection

Footings for slab foundations must be constructed to a depth below the prevailing ground level as shown in Figure II-1. The necessary depth of construction for these footings is based on the Borrego Valley Alluvial Fan Map.

The flood depth (D) shown for the particular location is converted to a construction depth (D_1) based on the velocity shown on the map, using the following table:

Velocity (V)	Construction Depth (D_1)
4 Feet/Second	$D_1 = D$
6 Feet/Second	$D_1 = D$
8 Feet/Second	$D_1 = 1.8 \times D$
Over 8 Feet/Second	Study Required

Where: D_1 = Depth Below Ground (Feet)
 D = Depth Shown on Alluvial Fan Map (Feet)
 V = Velocity Shown on Alluvial Map Map
(Feet/Second)

Erosion protection made of rock, gabions, or rip-rap must be installed to the depth D_1 .

SOURCE: BORREGO VALLEY
FLOOD MANAGEMENT
REPORTS

REQUALING USING HEC-18

SCORE INCLUDES BOTH GENERAL SCORE & LOCAL (PIER) SCORE

PIER SCORE, $y_s = y_1 \cdot 2 \cdot k_1 \cdot k_2 \cdot k_3 \cdot k_4 \left(\frac{\phi}{y_1} \right)^{0.65} F^{0.43}$ pg 21
HEC-18

WHERE: $k_1 = k_2 = k_4 = 1.0$

$k_3 = 1.1$

GENERAL SCORE, $\bar{y}_s = 1.2 y_1$ ASSUMING A STRAIGHT BED DEFORMATION
FOR 4-59 WRP

HEC-18 SUGGESTS $\bar{y}_s = 1.02 y_1$ FOR
BRAIDED STREAMS

SO USE $1.2 y_1$ FOR DAMPED PIERS

$2 y_1$ FOR CATCH WALLS

SO PIER SCORE, $y_s = 2.2 y_1 \left(\frac{\phi}{y_1} \right)^{0.65} F^{0.43}$

WHERE $\phi = 1 \text{ ft}$

REGIME MODEL	y_1	F	y_s	\bar{y}_s	$y_s + \bar{y}_s$	DETH CHANNEL
DMND	2.97	1.0	3.22	4.46	7.68	10.65
CARBAN	2.28	2.17	4.10	3.42	7.52	9.80
RANS HILL	0.98	1.89	2.87	1.47	4.34	5.32
COUNTRY	2-2 1/4	1.0	3.5	1.8-2.43	5.3-5.53	7.3-7.8



PROJECT NAME BORRERO SPRINGS SUBDIVISION DRAWN BY W. CRAMPDEN

CHECKED BY _____

PROJECT NUMBER 2418 DATE 7-12-06 PAGE 5 OF 19



U.S. Department
of Transportation

**Federal Highway
Administration**

Publication No. FHWA HI-96-031
November 1995

Hydraulic Engineering Circular No. 18

Evaluating Scour at Bridges

Third Edition



National Highway Institute

Office of Technology Applications, HTA-22
Federal Highway Administration
400 Seventh Street, S.W.
Washington, D.C. 20590

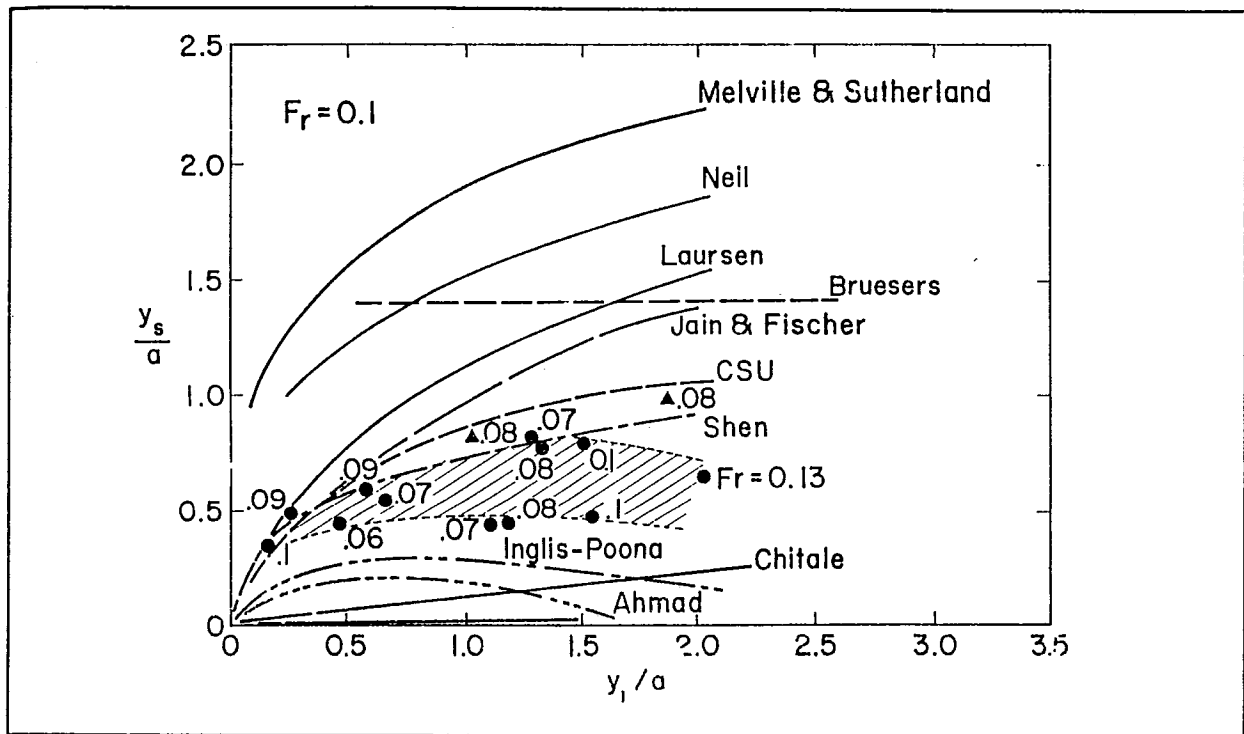


Figure 5. Comparison of scour equations with field scour measurements (after Jones).⁽⁴⁴⁾

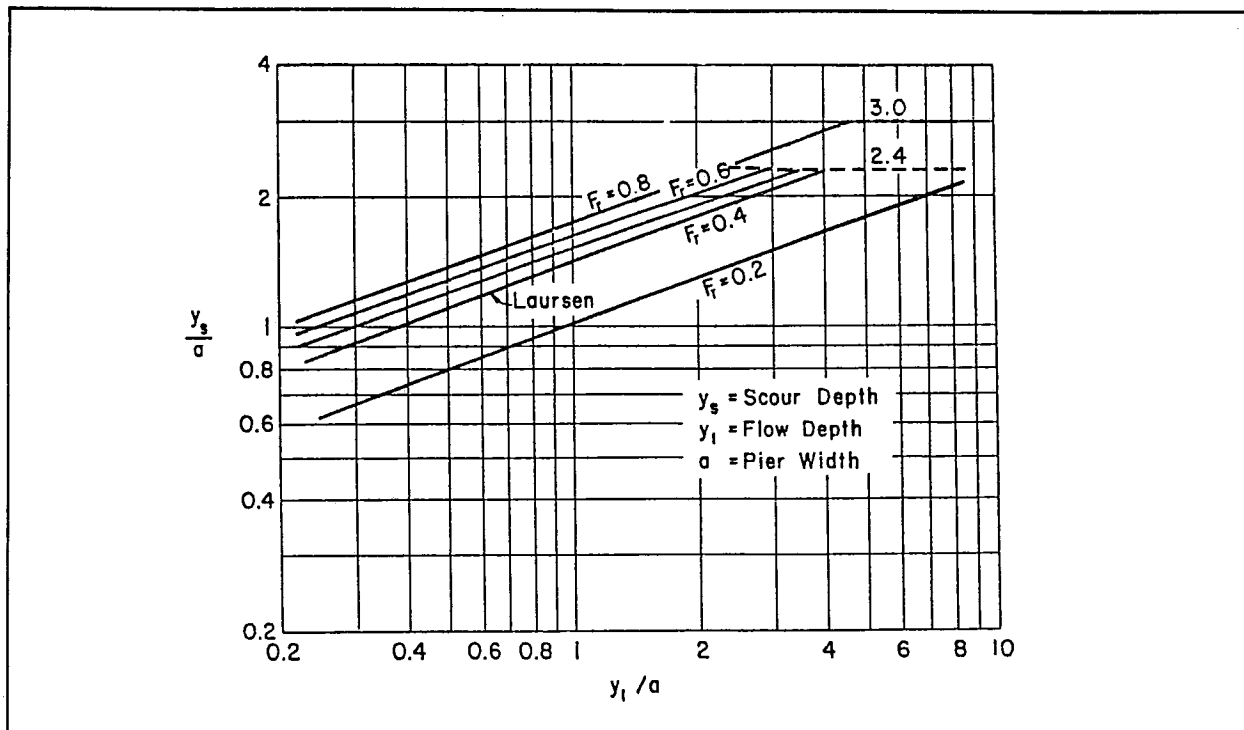


Figure 6. Values of y_s/a vs. y_l/a for CSU's equation.⁽⁴⁷⁾

Chang noted that in all the data he studied, there were no values of the ratio of scour depth to pier width (y_s/a) larger than 2.3.⁽⁴⁷⁾ From laboratory data, Melville and Sutherland reported 2.4 as an upper limit ratio for cylindrical piers.⁽²⁹⁾ In these studies, the Froude Number was less than 1.0. These upper limits were derived for circular piers and were uncorrected for pier shape and for skew. Also, pressure flow or debris can increase the ratio.

From the above discussion, the ratio of y_s/a can be as large as 3 at large Froude Numbers. Therefore, it is recommended that the maximum value of the ratio be taken as 2.4 for Froude Numbers less than or equal to 0.8 and 3.0 for larger Froude Numbers. These limiting ratio values apply only to round nose piers which are aligned with the flow.

Computing Pier Scour. To determine pier scour, an equation based on the CSU equation is recommended for both live-bed and clear-water pier scour.⁽¹³⁾ The equation predicts maximum pier scour depths. The equation is:

$$\frac{y_s}{y_1} = 2.0 K_1 K_2 K_3 K_4 \left[\frac{a}{y_1} \right]^{0.65} Fr_1^{0.43} \quad (21)$$

For round nose piers aligned with the flow:

$$\begin{aligned} y_s &\leq 2.4 \text{ times the pier width (a) for } Fr \leq 0.8 \\ y_s &\leq 3.0 \text{ times the pier width (a) for } Fr > 0.8 \end{aligned} \quad (21a)$$

In terms of y_s/a , equation 21 is:

$$\frac{y_s}{a} = 2.0 K_1 K_2 K_3 K_4 \left[\frac{y_1}{a} \right]^{0.35} Fr_1^{0.43} \quad (22)$$

where:

- y_s = Scour depth, m
- y_1 = Flow depth directly upstream of the pier, m
- K_1 = Correction factor for pier nose shape from figure 7 and table 2
- K_2 = Correction factor for angle of attack of flow from table 3 or equation 23
- K_3 = Correction factor for bed condition from table 4
- K_4 = Correction factor for armoring by bed material size from equation 24 and table 5
- a = Pier width, m
- L = Length of pier, m
- Fr_1 = Froude Number directly upstream of the pier = $V_1/(gy_1)^{1/2}$
- V_1 = Mean velocity of flow directly upstream of the pier, m/s
- g = Acceleration of gravity (9.81 m/s^2)

The correction factor for angle of attack of the flow K_2 given in table 3 can be calculated using the following equation:

$$K_2 = (\cos \theta + L/a \sin \theta)^{0.65} \quad (23)$$

If L/a is larger than 12, use $L/a = 12$ as a maximum in equation 23 and table 3.

Table 2. Correction Factor, K_1 , for Pier Nose Shape.	
Shape of Pier Nose	K_1
(a) Square nose	1.1
(b) Round nose	1.0
(c) Circular cylinder	1.0
(d) Group of cylinders	1.0
(e) Sharp nose	0.9

Table 3. Correction Factor, K_2 , for Angle of Attack, θ , of the Flow.			
Angle	$L/a=4$	$L/a=8$	$L/a=12$
0	1.0	1.0	1.0
15	1.5	2.0	2.5
30	2.0	2.75	3.5
45	2.3	3.3	4.3
90	2.5	3.9	5.0
Angle = skew angle of flow L = length of pier, m			

Table 4. Increase in Equilibrium Pier Scour Depths, K_3 , for Bed Condition.		
Bed Condition	Dune Height m	K_3
Clear-Water Scour	N/A	1.1
Plane bed and Antidune flow	N/A	1.1
Small Dunes	$3 > H \geq 0.6$	1.1
Medium Dunes	$9 > H \geq 3$	1.2 to 1.1
Large Dunes	$H \geq 9$	1.3

The correction factor K_4 decreases scour depths for armoring of the scour hole for bed materials that have a D_{50} equal to or larger than 0.06 m ($D_{50} \geq 0.06$ m). The correction factor results from recent research for FHWA by Molinas at CSU which showed that when the approach velocity (V_1) is less than the critical velocity (V_{c90}) of the D_{90} size of the bed material and there is a gradation in sizes in the bed material, the D_{90} will limit the scour depth.^(31,32) The equation developed by Jones from analysis of the data is:⁽²⁵⁾

$$K_4 = [1 - 0.89 (1 - V_R)^2]^{0.5} \quad (24)$$

where:

$$V_R = \left[\frac{V_1 - V_i}{V_{c90} - V_i} \right] \quad (24a)$$

$$V_i = 0.645 \left[\frac{D_{50}}{a} \right]^{0.053} V_{c50} \quad (24b)$$

V_R = Velocity ratio
 V_1 = Approach velocity, m/s
 V_i = Approach velocity when particles at a pier begin to move, m/s
 V_{c90} = Critical velocity for D_{90} bed material size, m/s
 V_{c50} = Critical velocity for D_{50} bed material size, m/s
 a = Pier width, m

$$V_c = 6.19 y^{1/6} D_c^{1/3} \quad (24c)$$

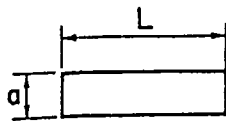
D_c = Critical particle size for the critical velocity V_c , m

Limiting K_4 values and bed material size are given in table 5.

Table 5. Limits for Bed Material Size and K_4 Values.			
Factor	Minimum Bed Material Size	Minimum K_4 Value	$V_R > 1.0$
K_4	$D_{50} \geq 0.06$ m	0.7	1.0

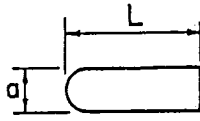
1. The correction factor K_1 for pier nose shape should be determined using table 2 for angles of attack up to 5 degrees. For greater angles, K_2 dominates and K_1 should be considered as 1.0. If L/a is larger than 12, use the values for $L/a = 12$ as a maximum in table 3 and equation 24.
2. The values of the correction factor K_2 should be applied only when the field conditions are such that the entire length of the pier is subjected to the angle of attack of the flow. Use of this factor directly from the table will result in a significant over-prediction of scour if (1) a portion of the pier is shielded from the direct impingement of the flow by an abutment or another pier; or (2) an abutment or another pier redirects the flow in a direction parallel to the pier. For such cases, judgment must be exercised to reduce the value of the K_2 factor by selecting the effective length of the pier actually subjected to the angle of attack of the flow.
3. The correction factor K_3 results from the fact that for plane-bed conditions, which is typical of most bridge sites for the flood frequencies employed in scour design, the maximum scour may be 10 percent greater than computed with equation 21. In the unusual situation where a dune bed configuration with large dunes exists at a site during flood flow, the maximum pier scour may be 30 percent greater than the predicted equation value. This may occur on very large rivers, such as the Mississippi. For smaller streams that have a dune bed configuration at flood flow, the dunes will be smaller and the maximum scour may be only 10 to 20 percent larger than equilibrium scour. For antidune bed configuration the maximum scour depth may be 10 percent greater than the computed equilibrium pier scour depth.

(24a)



(a) SQUARE NOSE

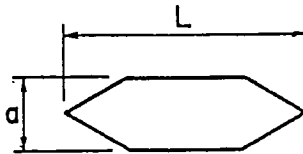
(24b)



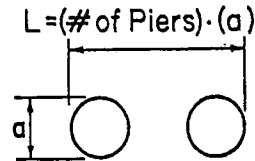
(b) ROUND NOSE



(c) CYLINDER



(d) SHARP NOSE

(e) GROUP OF CYLINDERS
(See Multiple Columns)

(24c)

Figure 7. Common pier shapes.

Pier Scour for Very Wide Piers. Flume studies on scour depths at wide piers in shallow flows indicate that even the CSU equation overestimates scour depth for this case.⁽⁴⁸⁾ Field observations of scour depths at bascule piers in shallow flows also suggest that the CSU equation overestimates scour depths. However, at the present time, there is insufficient information to estimate a decrease in scour depths given by the CSU equation for wide piers in shallow flow.

Pier Scour for Exposed Footings. Pier footings and/or pile caps may become exposed to the flow by scour. This may occur either from long-term degradation, contraction scour, or lateral shifting of the stream. Computations of local pier scour depths for footings or pile caps exposed to the flow based on footing or pile cap width appears to be too conservative. For example, calculations of scour depths for the Schoharie Creek bridge failure were closer to the measured model and prototype scour depths when pier width was used rather than footing width.⁽⁴⁹⁾ It appeared that the footing decreased the potential scour depth.

A model study of scour at the Acosta Bridge at Jacksonville, Florida, by Jones found that when the top of the footing was flush with the streambed, local scour was 20 percent less than for other conditions tested.⁽⁵⁰⁾ The other conditions were bottom of the footing at the bed surface, the top of the footing at the water surface with pile group exposed and top of footing at mid depth. In a generalized study, it was found that a footing extending upstream of the pier reduced pier scour when the top of the footing was located flush or below the bed, but scour holes became deeper and larger in proportion to the extent that the footing projected into the flow field.

Based on this study, the following recommendation was made for calculating pier scour if the footing is or may be exposed to the flow.

"It is recommended that the pier width be used for the value of 'a' in the pier scour equations if the top of the footing (or pile cap) is at or below the streambed (after taking into account long-term degradation and contraction scour). If the pier footing extends above the streambed, make a second computation using the width of the footing for the value of 'a' and the depth and average velocity in the flow zone obstructed by the footing for the 'y' and 'V' respectively in the scour equation. Use the larger of the two scour computations" (see figure 8).

If the top of the footing or pile cap is at the long-term degradation and/or contraction scour elevation, then it is only necessary to compute the scour depth considering the pier width.

EVALUATE DERIVS INDEXED SCORE

$$\frac{b_d}{T_d} = \frac{2.5\phi}{1.2\phi} = \frac{2.5'}{1.5'}$$

SEE APPENDIX B

$$b_e = \frac{0.52 T_d b_d + (y - 0.52 T_d) b}{y}$$

EG 6.22 WRP

$$b_e = \frac{1.95 + (y - 0.78)}{y}$$

REGIME MODEL	y_1	b_e	y_s^*	$y_s^* + y_s$	DESIGN LENGTH
DAWDY	2.97	1.39	3.99	8.45	11.42
CARAZON	2.28	1.51	5.35	8.77	11.05
RAMS HILL	0.98	2.19	4.78	6.25	7.23
CONWAY	2-2 1/4	—	3.5	5.3-5.53	2.3-2.8

THE CONWAY SPECIFIES A MINIMUM CLEAR SPACE OF 2-2 1/4 FT ABOVE EXISTING GRADE

CONSIDERING THE CLEAR SPACE SHOULD BE THE EVENLY GRADE LINE OR $y_1 + \frac{y_1^2}{2g}$

DAWDY	4.43'
CARAZON	7.62'
RAMS HILL	2.73'
CONWAY	2-2 1/4'

USE 3 FT FOR DESIGN SINCE DAWDY & CARAZON HAVE FLUWS & THE CONWAY SPECIFIES 2 1/4'



PROJECT NAME BORRERO SPRINGS SUBDIVISION DRAWN BY W. CRAMPON
 CHECKED BY _____
 PROJECT NUMBER 2418 DATE 2-12-06 PAGE 12 OF 19

SCOUR ANALYSIS SUMMARY

DESIGN SCOUR DEPTH, $y_{\text{DES}} = \text{GENERAL SCOUR} + \text{PIER SCOUR}$

$$\begin{aligned} \text{GENERAL SCOUR, } \bar{y} &= 1.5 y_1 \\ &= 1 \text{ to } 2 y_1 \\ &= 0.7 y_1 \end{aligned}$$

OF 4-59 WRP
HEC-18
CONV. METHOD

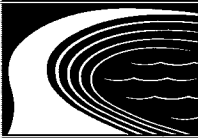
$$\begin{aligned} \text{PIER SCOUR, } y_s &= f(y_1, \phi, F, \text{SKEWLINE}) \\ &= f(V, \phi) \end{aligned}$$

HEC-18
CONV. METHOD

FOR GENERAL SCOUR & PIERS, USE $1\frac{1}{2} y_1$
* CHECK w/ CONV. METHOD

REGIME MODEL	y_1	V	F	y_s	y_s^*	\bar{y}	y_{DES}
DAWDY	2.97	9.70	1	3.22	3.79	4.46	8.45
CARZON	2.28	18.54	2.17	4.14	5.35	3.42	8.77
RAMSILL	0.98	10.61	1.89	2.87	4.78	1.27	6.25
CONV.	2.2 1/4	6 1/2 - 7	1	3.5	3.5	1.8 - 2.03	3.3 - 5.53

TerraCosta



Consulting Group

PROJECT NAME BERRIO SPRINGS SUBDIVISION

DRAWN BY W. CRAMPIN

CHECKED BY _____

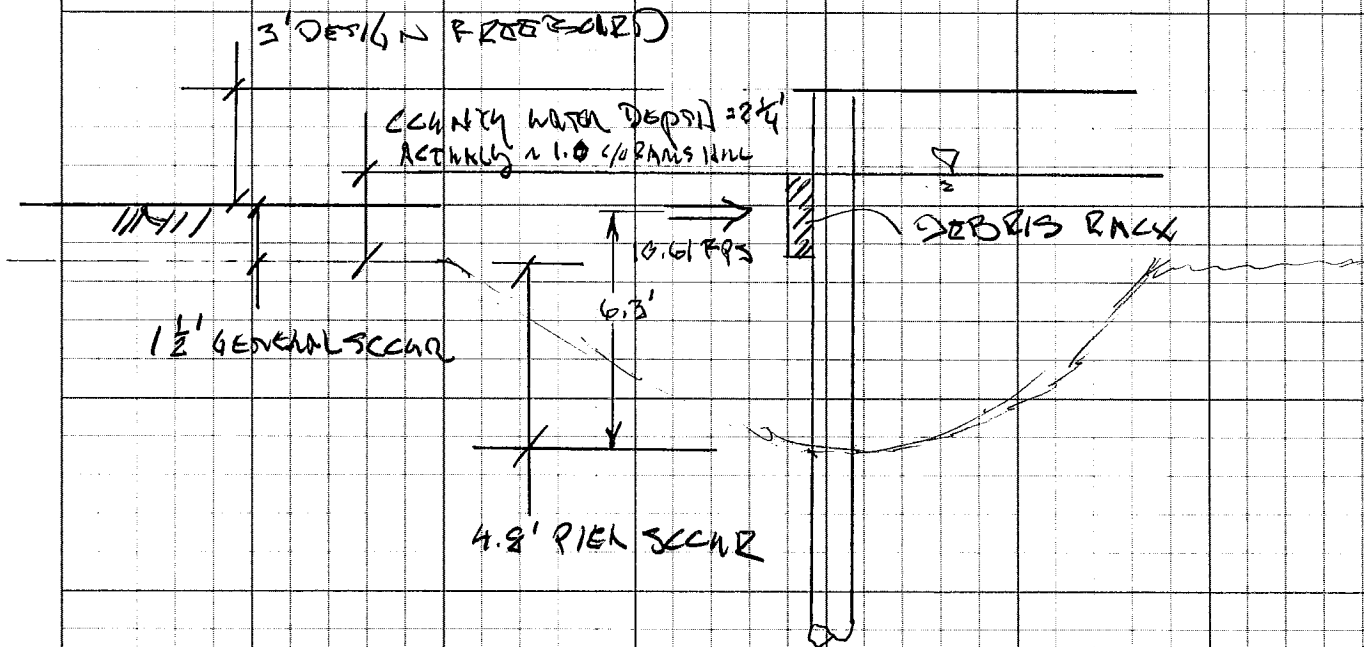
PROJECT NUMBER 2418

DATE 7-12-06

PAGE 13 OF 19

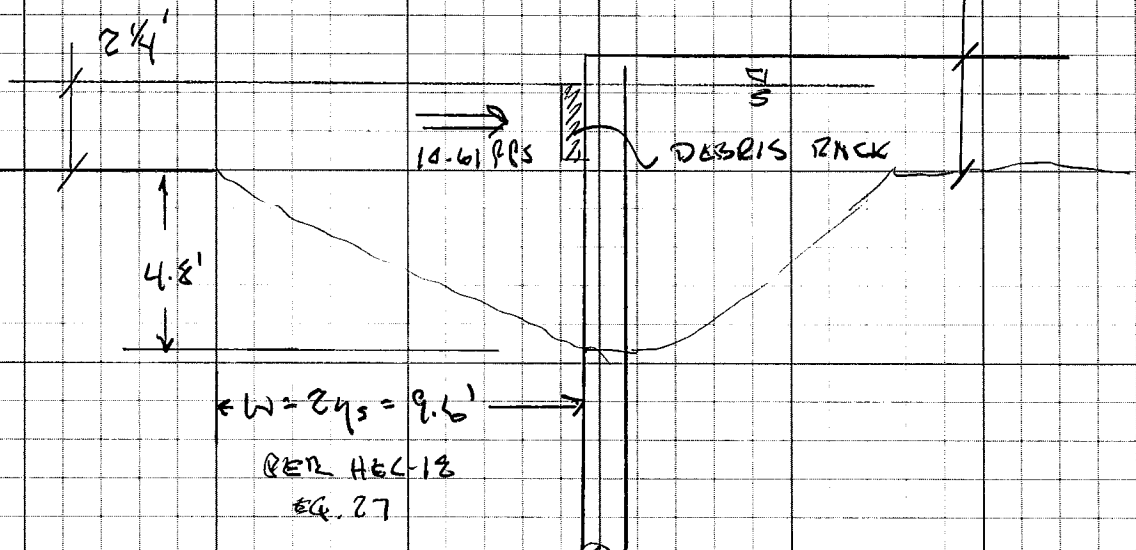
USING 3 FT. FLOOD CLEARANCE & THE RAMS HLM MODEL
 \therefore DESIGN CANTILEVER = 9.25 FT > 7.8 FT COUNTY REQUIREMENT
 OR 19% ABOVE COUNTY REQUIREMENTS

CASE 1 w/ 1 1/2' GENERAL SCOUR



CASE 2 w/ 0.45' GENERAL SCOUR

3' DESIGN FREEBOARD



PROJECT NAME BORRELO SPRINGS SUBDIVISION DRAWN BY W. CRAMPIN
 CHECKED BY _____
 PROJECT NUMBER 2418 DATE 7-12-06 PAGE 14 OF 19

Width of Scour Holes. The topwidth of a scour hole in cohesionless bed material from one side of a pier or footing can be estimated from the following equation:⁽⁵⁶⁾

$$W = y_s (K + \cot \theta) \quad (27)$$

where:

- W = Topwidth of the scour hole from each side of the pier or footing, m
- y_s = Scour depth, m
- K = Bottom width of the scour hole as a fraction of scour depth
- θ = Angle of repose of the bed material ranging from about 30° to 44°

The angle of repose of cohesionless material in air ranges from about 30° to 44° . Therefore, if the bottom width of the scour hole is equal to the depth of scour y_s ($K = 1$), the topwidth in cohesionless sand would vary from 2.07 to $2.80 y_s$. At the other extreme, if $K = 0$, the topwidth would vary from 1.07 to $1.8 y_s$. Thus, the topwidth could range from 1.0 to $2.8 y_s$ and will depend on the bottom width of the scour hole and composition of the bed material. In general, the deeper the scour hole, the smaller the bottom width. In water, the angle of repose of cohesionless material is less than the values given for air; therefore, a topwidth of $2.0 y_s$ is suggested for practical applications (figure 13).

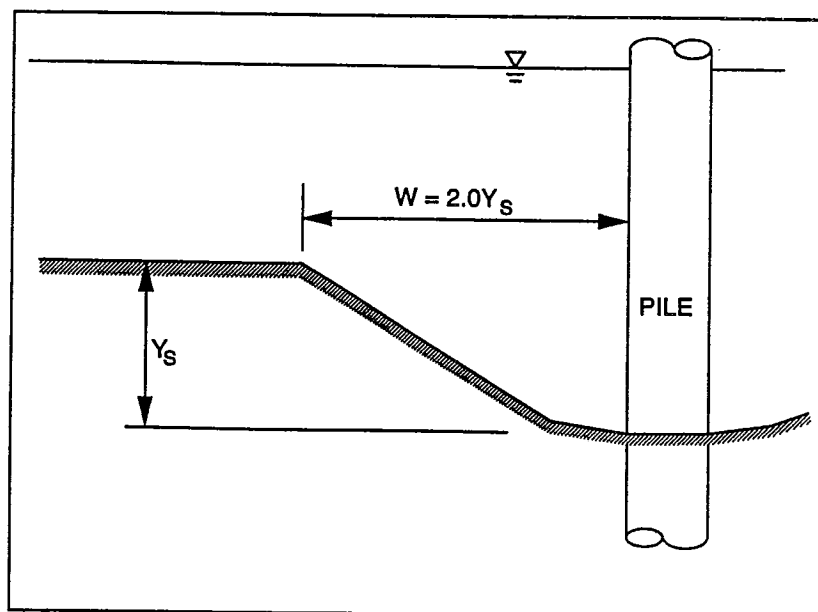


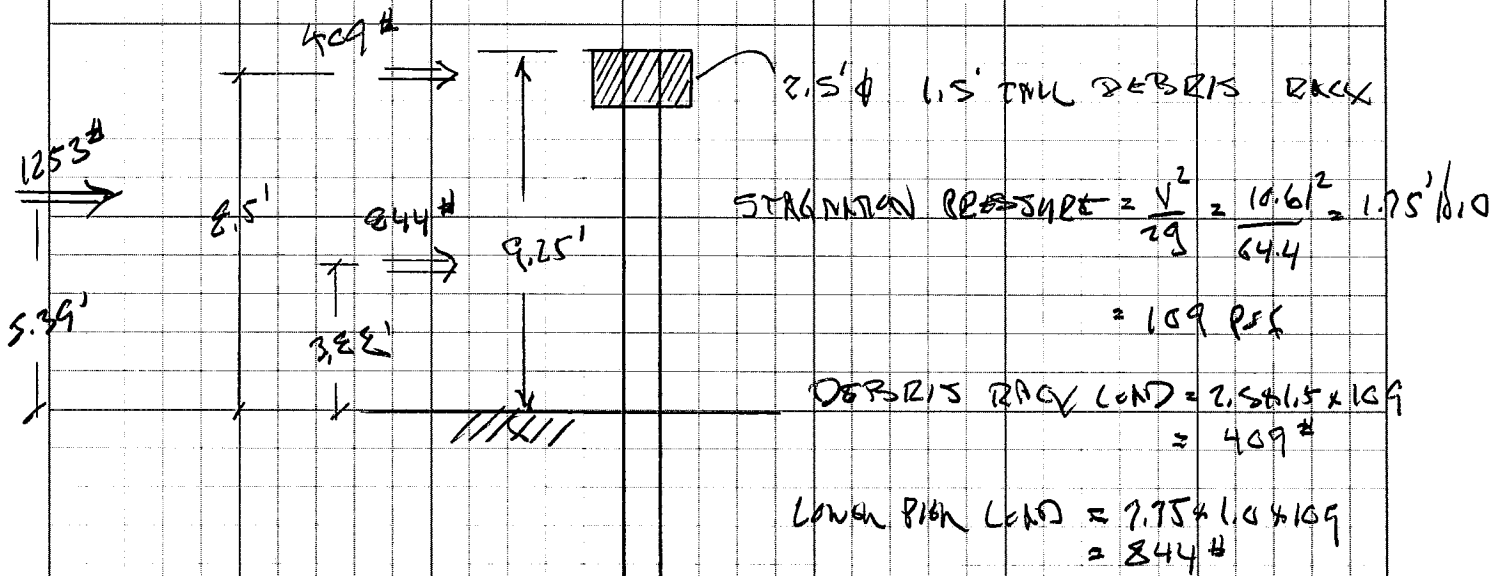
Figure 13. Topwidth of scour hole.

4.3.6 Step 6: Local Scour at Abutments

General. Local scour occurs at abutments when the abutment obstructs the flow. The obstruction of the flow forms a horizontal vortex starting at the upstream end of the abutment and running along the toe of the abutment, and a vertical wake vortex at the downstream end of the abutment. The vortex at the toe of the abutment is very similar to the horseshoe vortex that forms at piers, and the vortex that forms at the downstream end is similar to the wake vortex that forms downstream of a pier, or that forms downstream of any flow separations. Research has been conducted to determine the depth and location of the scour hole that develops for the horizontal (so called horseshoe) vortex that occurs at the upstream end of the abutment, and numerous abutment scour equations have been developed to predict this scour depth. However, abutment failures and

FOR DESIGN USE THE 9.25' CANTILEVER AS PER THE COUNTY DESIGN APPROACH

NOTE: THIS COMBINES BOTH LOCAL (PIER) SCOUR & GENERAL SCOUR THEN ADDS THE WATER DEPTH TO THIS COMBINED VALUE

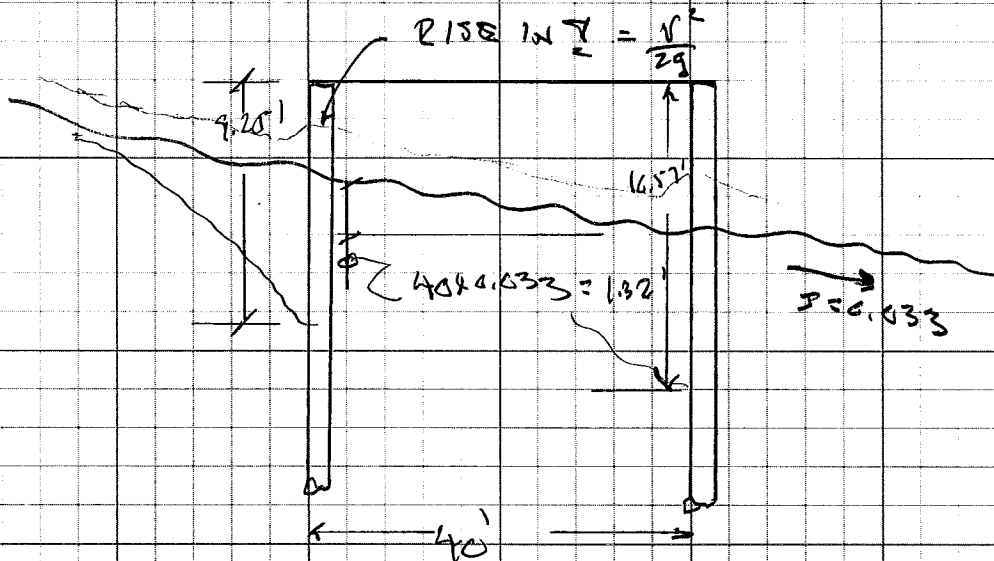


$$\bar{Q} = \frac{409 \times 8.5 + 844 \times 3.88}{409 + 844} = 5.39' \quad w/P = 409 + 844 = 1253 \#$$

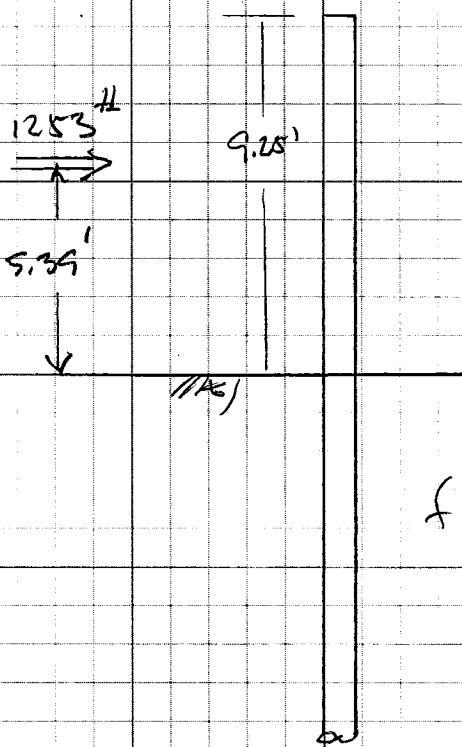
$$O.D. M = 539 \times 1253 = 6,754 \text{ FT-LB}$$

REQUIRE A DAMPING COEFFICIENT

ASSUME DAMPING DISTANCE = 40'



NOTE: PIER LOADS ARE THE SAME ONLY THERE IS MORE FLOODING ON THE DOWNSTREAM PIER



REF: MIT LOCK & RESS DM 7.02

$$T = \left(\frac{E I}{K} \right)^{1/4} = \left(\frac{3 \times 10^4 \times \frac{\pi \times 12^4}{4}}{40} \right)^{1/4} = 37.7'' = 3.14' \text{ ft}$$

$$M = 6754 \text{ ft-lb} \quad \text{FOR 100 WIND} \quad M = 8,720 \text{ ft-lb}$$

$$f_b = \frac{M C}{I} = \frac{M}{S}$$

$$f = 40 \text{ psi}$$

$$REF S = \frac{M}{0.66 f_y} = \frac{8720 \times 12''}{24000} = 4.36 \text{ in}^3$$

$$\text{USE } M 4 \times 13 \text{ I-Beam w/ } S = 3.24 \text{ in}^3$$

$$\therefore f_b = 19,910 \text{ psi} = 0.55 f_y < 0.66 f_y$$

TerraCosta



PROJECT NAME BORRHO SPRINGS SUBDIVISION

DRAWN BY W. CRAMPTON

CHECKED BY _____

PROJECT NUMBER 2418

DATE 7-12-06

PAGE 17 OF 19

Laterally Loaded Pile Analysis -- Borrego Springs Subdivision -- 7/1/2006									
Circular Piles w/LT=4									
Reese & Matlock solution - DM7.02									
Pile Moment of Inertia, I (in ⁴):									
Pile Diameter, D (in):									
Pile Modulus, E (psi):									
Soil Modulus, f (psi):									
Ultimate lateral soil capacity ref. Brom's 1984									
Pult=0.5*soil-density*D ^{1.3} *Kp/(H+L) for LT<2									
Pult=M/(H+0.54(P/soil-density*D*Kp) ^{0.5}) for LT>4									
Unsupported Cantilevered Height, H (ft):									
Depth of Embedment, L (ft):									
Soil phi, degrees									
Soil density, pcf									
Effective Depth, T (in):									
Effective Depth, T (ft):									
Lateral Load, P (kips):									
Load Induced Moment, M (kip-ft):									
Embedment Depth Ratio, LT:									
Computation of Variation in Soil Induced Moment with LT = 4									
Depth, T	Depth, ft	Fdm	Fdp	Mmm	Mpt	Mtotal	Fiber Bending, Fb (psi)		
0.00	0.00	1.000	0.000	6.75	0.00	6.75	478		
0.25	0.79	0.992	0.240	6.70	0.95	7.64	541		
0.50	1.57	0.970	0.467	6.55	1.84	8.39	593		
0.75	2.36	0.928	0.627	6.25	2.47	8.72	617		
1.00	3.14	0.859	0.732	5.80	2.88	8.68	614		
1.25	3.93	0.753	0.767	5.09	3.02	8.11	573		
1.50	4.71	0.640	0.747	4.32	2.94	7.26	514		
Computation of Pile Deformation with LT = 4									
Depth, T	Depth, ft	Fdm	Fdp	DEF.m	DEF.pt	DEF tot."	SLOPE	Top of Pile Def (in)	
0.00	0.00	1.56	2.50	0.06	0.06	0.11"	0.00264268	0.32"	
0.25	0.79	1.16	2.07	0.04	0.05	0.09"	0.00240329		
0.50	1.57	0.82	1.65	0.03	0.04	0.07"	0.002073927		
0.75	2.36	0.52	1.30	0.02	0.03	0.05"	0.001666646		
1.00	3.14	0.30	0.97	0.01	0.02	0.03"	0.001370484		
1.25	3.93	0.12	0.67	0.00	0.01	0.02"	0.000821935		
1.50	4.71	0.03	0.44	0.00	0.01	0.01"			
NOTE: Top of pile deflection is the combination of:									
Ground surface deflection, DEF tot." PLUS									
Deflected pile due to angular rotation only, slope*Ht. PLUS									
Deflected pile due to loading, PL ³ /3EI									
where: L=lever arm									

ASSUMING A M 4 X 13.5 BEAM IN / S = 5.241.7
 11.4160 = FBS = 36,000 X 5.24 = 15.7 k.k.
 12 1/4" X 1000 3/4"

11.49 SOIL INDUCED MOMENT = 8.72 k-ft

NOTE: This spreadsheet is for a cantilevered pile with a horizontal load at the top. Thus, the calculated deflection is for a point 3.86 feet (9.25 - 5.39 = 3.86 feet) below the top of the drilled pier

SEISMIC LOADING

ALTHOUGH THE 12" ϕ DRILLED PILE HAS MORE CAPACITY THAN NEEDED WHEN REINFORCED WITH A #4 @ 13" ϕ BEAM

LIMIT WIND & SEISMIC LOADING TO THE SAME LOADS AS THE PILE INDICATED LOADING

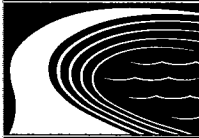
$$\therefore \text{DESIGN WIND/SEISMIC MOMENT} = 6,755 \text{ ft} \cdot \text{ft}$$

SINCE WIND & SEISMIC LOADS TAKEN AT ELEVATION DURING PILE DESIGN

ASSUME DESIGN STRENGTH = 4 FT TO ACCOUNT FOR VARIABILITY IN GROUND SURFACE BETA COEFFICIENT AND DESIGN CONCENTRATION

$$\therefore \text{DESIGN WIND/SEISMIC LOADING} = \frac{6755}{4} = 1689 \text{ ft} \cdot \text{ft}$$

SM 1650 ft/PILE



APPENDIX B

DEBRIS LOADING DESIGN CRITERIA

in which $(d_s + H_b)$ represents the flow depth beneath the bridge. The equation is very similar to an expression given by Gill (1981) for (horizontal) clear-water contraction scour, refer (5.7) in Section 5.1.1.

6.4.2. Effect of Debris

During floods, many rivers carry appreciable quantities of floating debris such as branches and roots of trees. If the debris becomes caught at bridge piers and abutments, it can accumulate into large masses of material normally referred to as debris rafts. A foundation with accumulated material causes a larger obstruction to the flow than without debris; the additional flow obstruction generally causes local scour depths in excess of depths under conditions without debris accumulation. The presence of large accumulations of debris was a significant factor in the failure of Wairoa River Road Bridge (Case Study A.4), Mangaheia No. 2 Road Bridge (Case Study B.1) and Mangaheia No. 5 Road Bridge (Case Study B.2).

The likelihood for debris accumulation at bridge foundations depends on a number of factors, including the availability of debris material, the potential for such material to be washed into streams and rivers, and the shape of the bridge foundations. In a study of woody debris transport in a Tennessee river, Diehl and Bryan (1993) found that the predominant large debris type comprised tree trunks with attached root masses. Such trees usually fall into a river because of bank erosion. Hence bank instability is an important catchment characteristic in identifying basins with a high potential for abundant production of debris.

McClellan (1994) found, using small-scale laboratory models, that debris accumulations could be formed such that they extend from the water surface to the streambed in all flow conditions. Under low Froude number conditions, the debris rafts tended to be shallow and extensive in plan area, while under high Froude number conditions, the debris rafts tended to be deep and narrow.

A device to deflect debris away from a bridge pier is described by Saunders and Oppenheimer (1993). The deflector, which is designed to generate counter-rotating streamwise vortices in its wake, is positioned so that the vortices migrate to the surface of the water ahead of the pier. The near-surface flow induced by the vortices is intended to deflect any debris safely around the pier.

Dongol (1989) and Melville and Dongol (1992) reported a laboratory study of local scour depths at circular bridge piers with debris rafts. The debris was modelled as an impervious circular cylinder, concentric to the pier and having its upper surface at the water surface level. They proposed the following expression for the equivalent size b_e of the uniform circular pier that induces about the same scour depth as the actual pier with accumulated debris:

$$b_e = \frac{0.52T_d b_d + (y - 0.52T_d)b}{y} \quad (6.22)$$

where T_d and b_d = thickness (vertical dimension) and width of the floating debris raft; and b = pier width, as shown in Figure 6.35. The equivalent width can therefore be used to estimate local scour depth where debris is present, if the dimensions of the likely debris accumulation can be estimated. Figure 6.35 also shows trends in the data. For the study, T_d/b varied from 0.52 to 1.64, while b_d/b varied from 2.1 to 6.9. The maximum local scour depth recorded was 3.6, representing a 50% increase over that at a uniform circular pier ($d_s=2.4b$). The maximum scour depths occurred when the debris raft extended to about the undisturbed bed level, that is, $T_d/b \approx 1$. Although derived from data for circular piers and debris masses, (6.22) can be applied to other pier shapes.

6.4.3. Local Scour in Layered Sediments

Many sedimentary deposits are heterogeneous and often distinct layers are present. If a more resistant layer underlies a readily erodible layer, scouring is inhibited and lesser scour depths

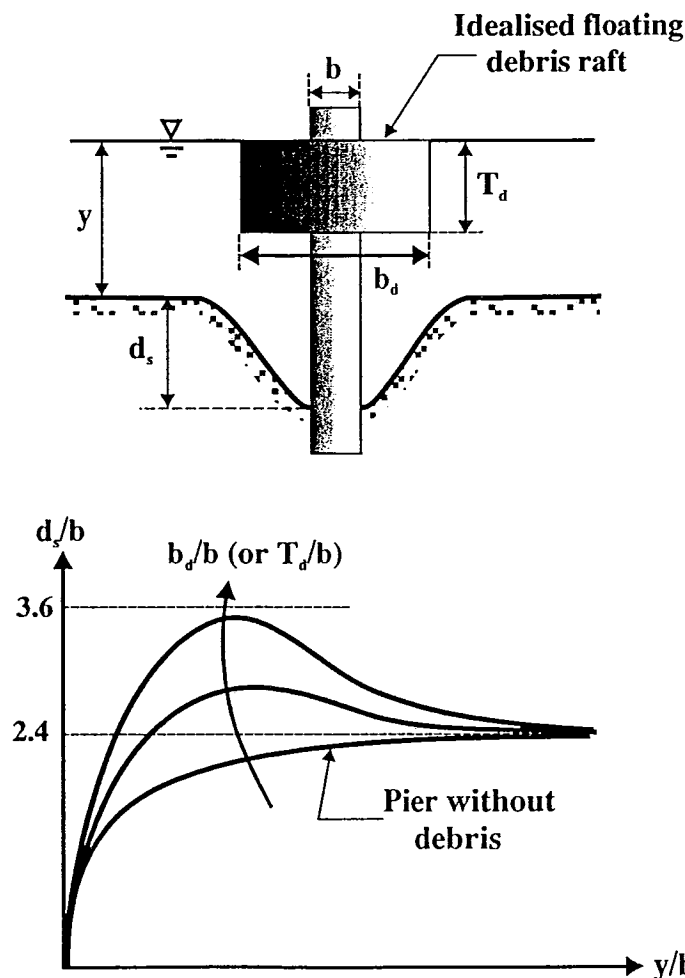


Figure 6.35. Local scour depth variation with quantity of floating debris.

develop than
the sediments c
was partly at
level stratum. Et
cases of coars

- Case I, scour p
- For Cas of the l distance to the r (1980) that for
- For Ca leaving of this (1991)

where y
upstream
respect
local sc

- For Ca the pier the sco being n

6.4.4. Local
The flow at bridge
develops alternate
situations as for ri
some of the mater
phase. For this
Breusers' (1965) e
depths measured a
from surge, the
subject to tidal flu

APPENDIX C

FOUNDATIONS AND EARTH STRUCTURES

NAVFAC DM 7.02

Naval Facilities Engineering Command

200 Stovall Street
Alexandria, Virginia 22332-2300

APPROVED FOR PUBLIC RELEASE



Foundations & Earth Structures

DESIGN MANUAL 7.02
REVALIDATED BY CHANGE 1 SEPTEMBER 1986

Section 7. LATERAL LOAD CAPACITY

1. **DESIGN CONCEPTS.** A pile loaded by lateral thrust and/or moment at its top, resists the load by deflecting to mobilize the reaction of the surrounding soil. The magnitude and distribution of the resisting pressures are a function of the relative stiffness of pile and soil.

Design criteria is based on maximum combined stress in the piling, allowable deflection at the top or permissible bearing on the surrounding soil. Although 1/4-inch at the pile top is often used as a limit, the allowable lateral deflection should be based on the specific requirements of the structure.

2. DEFORMATION ANALYSIS - SINGLE PILE.

a. General. Methods are available (e.g., Reference 9 and Reference 31, Non-Dimensional Solutions for Laterally Loaded Piles, with Soil Modulus Assumed Proportional to Depth, by Reese and Matlock) for computing lateral pile load-deformation based on complex soil conditions and/or non-linear soil stress-strain relationships. The COM 622 computer program (Reference 32, Laterally Loaded Piles: Program Documentation, by Reese) has been documented and is widely used. Use of these methods should only be considered when the soil stress-strain properties are well understood.

Pile deformation and stress can be approximated through application of several simplified procedures based on idealized assumptions. The two basic approaches presented below depend on utilizing the concept of coefficient of lateral subgrade reaction. It is assumed that the lateral load does not exceed about 1/3 of the ultimate lateral load capacity.

b. Granular Soil and Normally to Slightly Overconsolidated Cohesive Soils. Pile deformation can be estimated assuming that the coefficient of subgrade reaction, K_h , increases linearly with depth in accordance with:

$$K_h = \frac{fz}{D}$$

where: K_h = coefficient of lateral subgrade reaction (tons/ft³)

f = coefficient of variation of lateral subgrade reaction
(tons/ft³)

z = depth (feet)

D = width/diameter of loaded area (feet)

Guidance for selection of f is given in Figure 9 for fine-grained and coarse-grained soils.

c. Heavily Overconsolidated Cohesive Soils. For heavily overconsolidated hard cohesive soils, the coefficient of lateral subgrade reaction can be assumed to be constant with depth. The methods presented in Chapter 4 can be used for the analysis; K_h varies between $35c$ and $70c$ (units of force/length³) where c is the undrained shear strength.

d. Loading Conditions. Three principal loading conditions are illustrated with the design procedures in Figure 10, using the influence diagrams of Figure 11, 12 and 13 (all from Reference 31). Loading may be limited by allowable deflection of pile top or by pile stresses.

Case I. Pile with flexible cap or hinged end condition. Thrust and moment are applied at the top, which is free to rotate. Obtain total deflection, moment, and shear in the pile by algebraic sum of the effects of thrust and moment, given in Figure 11.

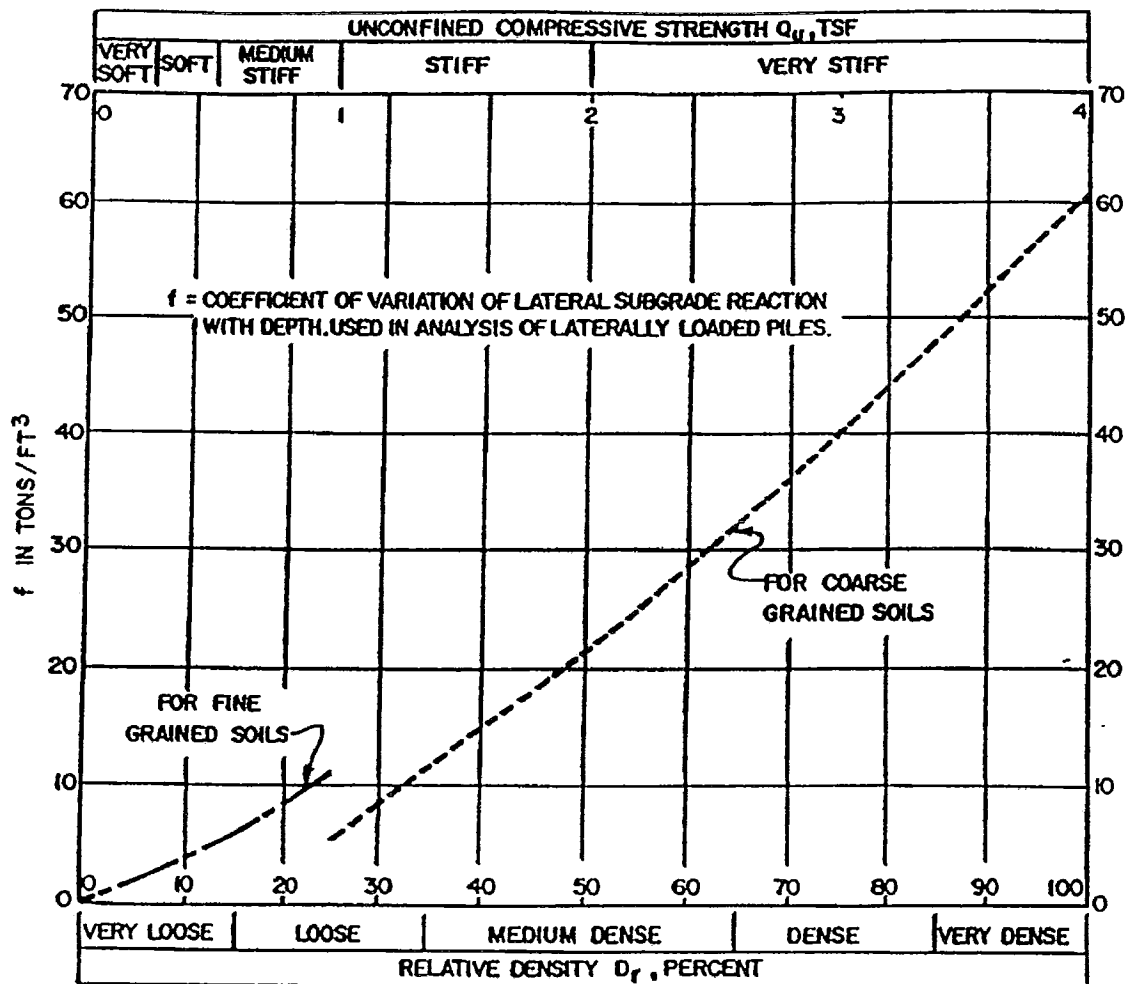


FIGURE 9
Coefficient of Variation of Subgrade Reaction

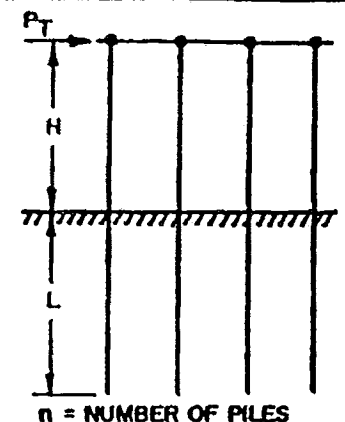
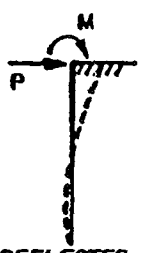
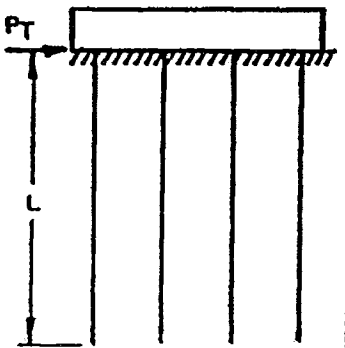

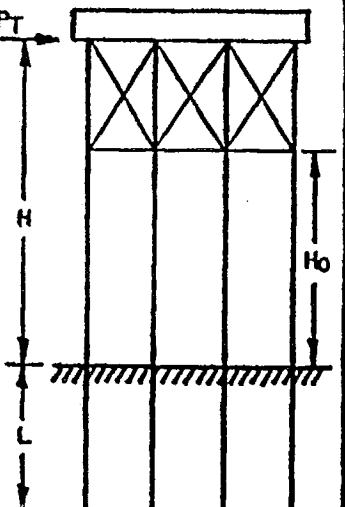
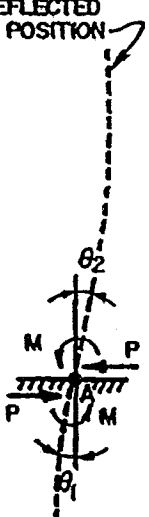
CASE I. FLEXIBLE CAP, ELEVATED POSITION		
CONDITION	LOAD AT GROUND LINE	DESIGN PROCEDURE
 <p>$n = \text{NUMBER OF PILES}$</p>	<p>FOR EACH PILE:</p> $P = \frac{P_T}{n}$ $M = PH$  <p>DEFLECTED POSITION</p>	<p>FOR DEFINITION OF PARAMETERS SEE FIGURE 12</p> <ol style="list-style-type: none"> 1. COMPUTE RELATIVE STIFFNESS FACTOR. $T = \left(\frac{EI}{f} \right)^{1/5}$ 2. SELECT CURVE FOR PROPER $\frac{L}{T}$ IN FIGURE 11. 3. OBTAIN COEFFICIENTS F_δ, F_M, F_V AT DEPTHS DESIRED. 4. COMPUTE DEFLECTION, MOMENT AND SHEAR AT DESIRED DEPTHS USING FORMULAS OF FIGURE 11. <p>NOTE: "f" VALUES FROM FIGURE 9 AND CONVERT TO LB/IN³.</p>
CASE II. PILES WITH RIGID CAP AT GROUND SURFACE		
		<ol style="list-style-type: none"> 1. PROCEED AS IN STEP 1, CASE I. 2. COMPUTE DEFLECTION AND MOMENT AT DESIRED DEPTHS USING COEFFICIENTS F_δ, F_M AND FORMULAS OF FIGURE 12. 3. MAXIMUM SHEAR OCCURS AT TOP OF PILE AND EQUALS $P = \frac{P_T}{n}$ IN EACH PILE.
CASE III. RIGID CAP, ELEVATED POSITION		
	<p>DEFLECTED POSITION</p> 	<ol style="list-style-type: none"> 1. ASSUME A HINGE AT POINT A WITH A BALANCING MOMENT M APPLIED AT POINT A. 2. COMPUTE SLOPE θ_2 ABOVE GROUND AS A FUNCTION OF M FROM CHARACTERISTICS OF SUPERSTRUCTURE. 3. COMPUTE SLOPE θ_1 FROM SLOPE COEFFICIENTS OF FIGURE 13 AS FOLLOWS: $\theta_1 = F_\theta \left(\frac{PT^2}{EI} \right) + F_\theta \left(\frac{MT}{EI} \right)$ 4. EQUATE $\theta_1 = \theta_2$ AND SOLVE FOR VALUE OF M. 5. KNOWING VALUES OF P AND M, SOLVE FOR DEFLECTION, SHEAR, AND MOMENT AS IN CASE I. <p>NOTE: IF GROUND SURFACE AT PILE LOCATION IS INCLINED, LOAD P TAKEN BY EACH PILE IS PROPORTIONAL TO $1/H_0^3$.</p>

FIGURE 10
Design Procedure for Laterally Loaded Piles

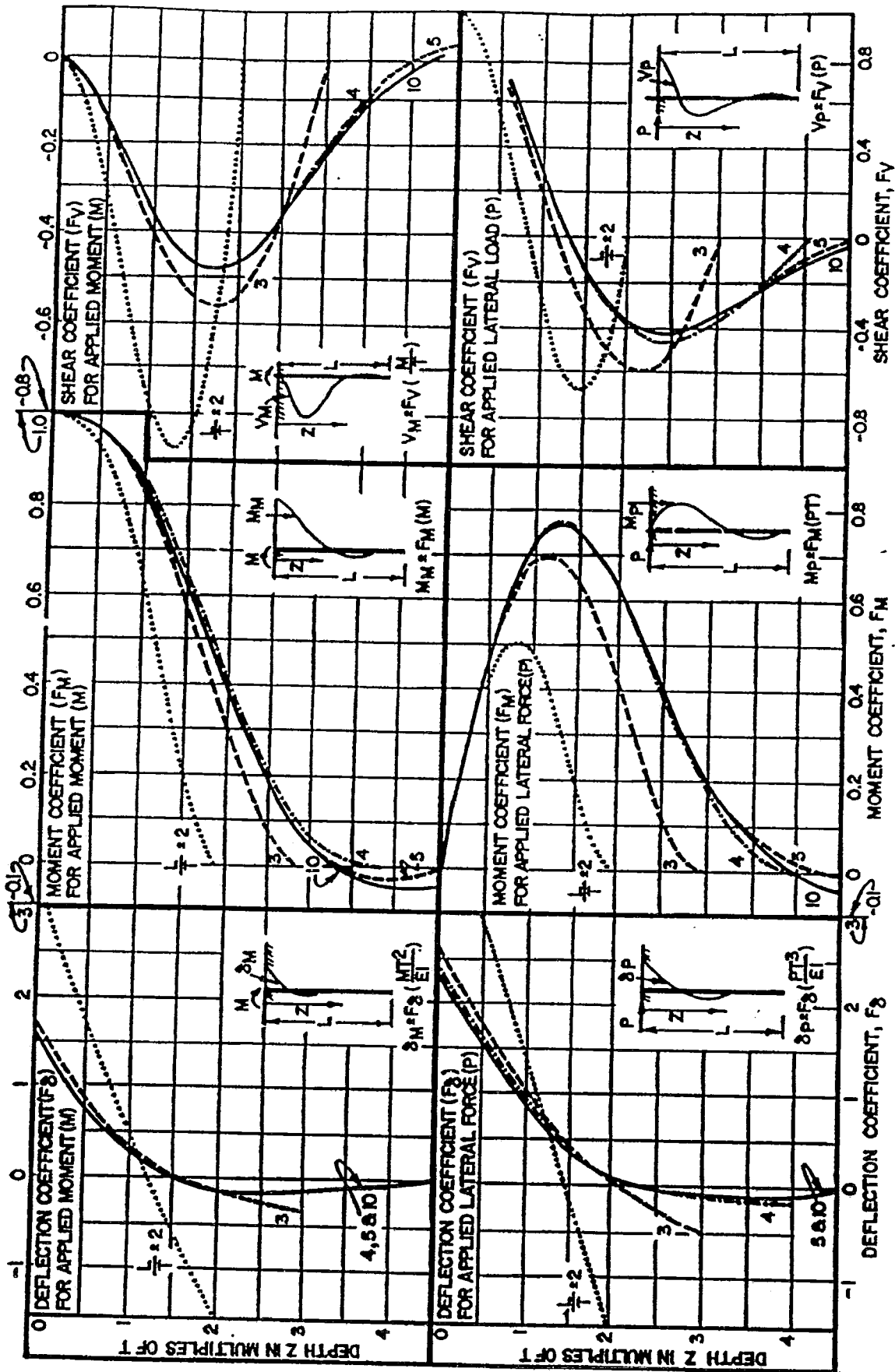


FIGURE 11
Influence Values for Pile with Applied Lateral Load and Moment
(Case I. Flexible Cap or Hinged End Condition)

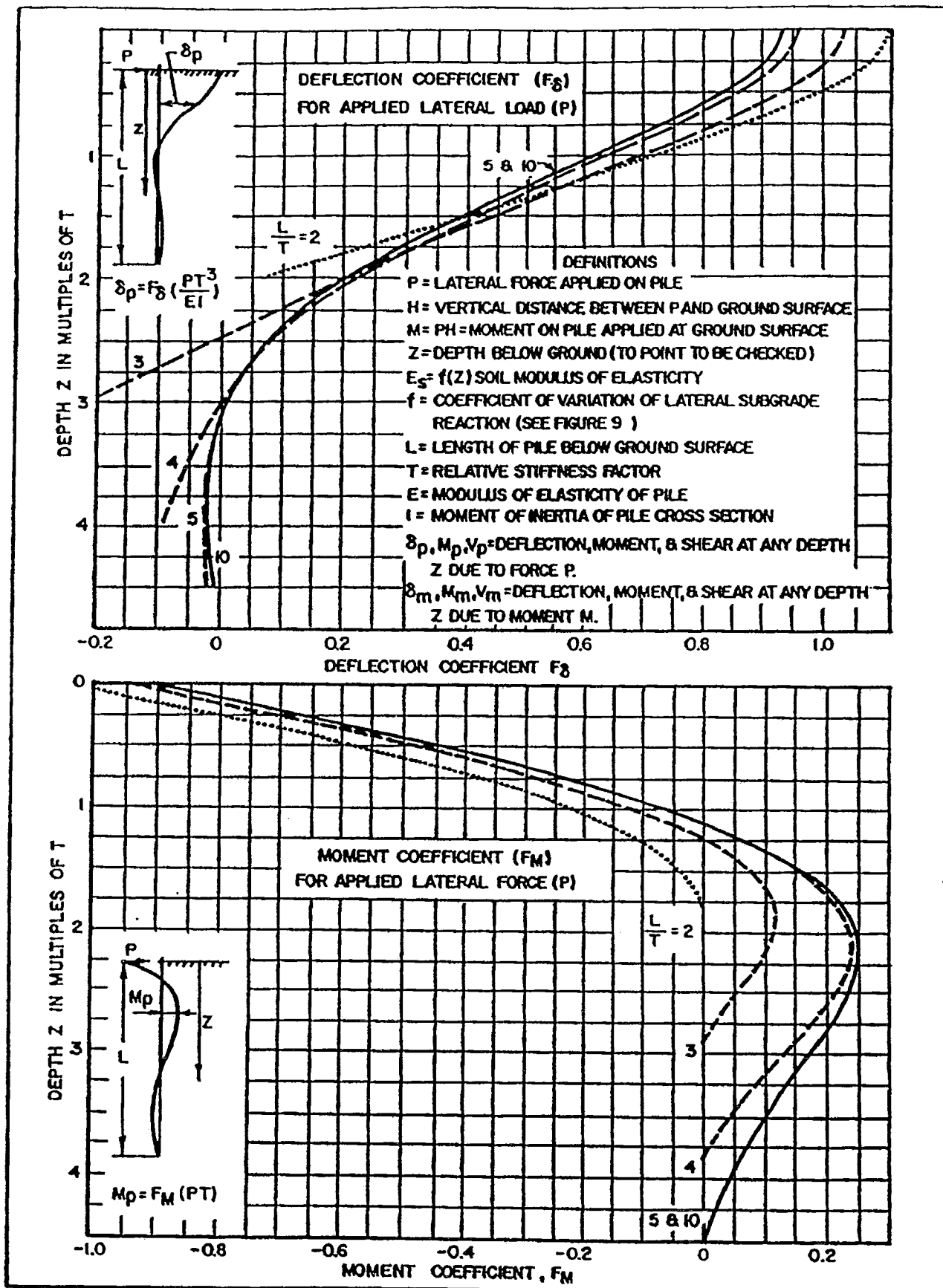


FIGURE 12
Influence Values for Laterally Loaded Pile
(Case II. Fixed Against Rotation at Ground Surface) ---
7.2-239

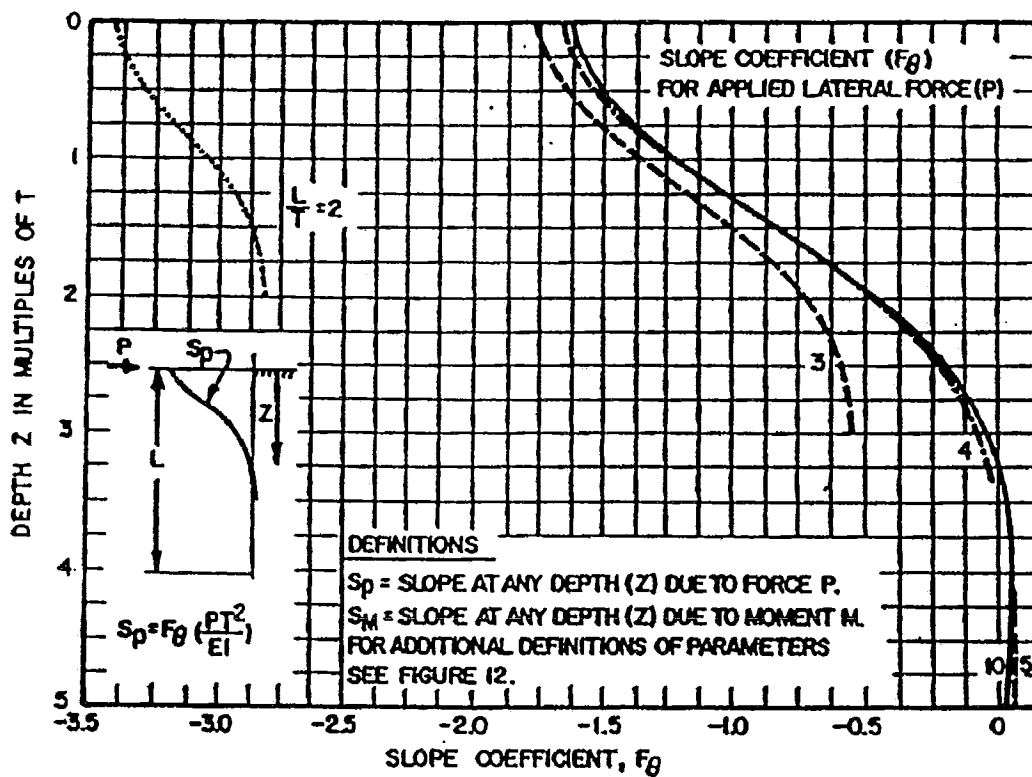
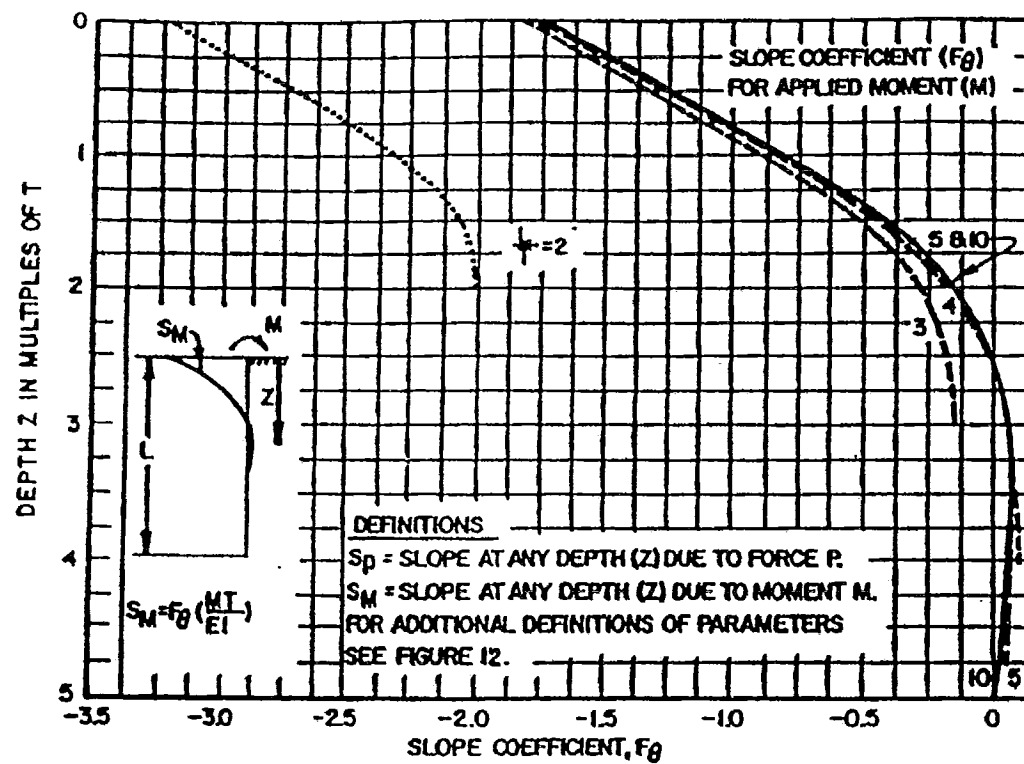


FIGURE 13
 Slope Coefficient for Pile with Lateral Load or Moment

Case II. Pile with rigid cap fixed against rotation at ground surface. Thrust is applied at the top, which must maintain a vertical tangent. Obtain deflection and moment from influence values of Figure 12.

Case III. Pile with rigid cap above ground surface. Rotation of pile top depends on combined effect of superstructure and resistance below ground. Express rotation as a function of the influence values of Figure 13 and determine moment at pile top. Knowing thrust and moment applied at pile top, obtain total deflection, moment and shear in the pile by algebraic sum of the separate effects from Figure 11.

3. CYCLIC LOADS.

Lateral subgrade coefficient values decrease to about 25% the initial value due to cyclic loading for soft/loose soils and to about 50% the initial value for stiff/dense soils.

4. LONG-TERM LOADING. Long-term loading will increase pile deflection corresponding to a decrease in lateral subgrade reaction. To approximate this condition reduce the subgrade reaction values to 25% to 50% of their initial value for stiff clays, to 20% to 30% for soft clays, and to 80% to 90% for sands.

5. ULTIMATE LOAD CAPACITY - SINGLE PILES. A laterally loaded pile can fail by exceeding the strength of the surrounding soil or by exceeding the bending moment capacity of the pile resulting in a structural failure. Several methods are available for estimating the ultimate load capacity.

The method presented in Reference 33, Lateral Resistance of Piles in Cohesive Soils, by Broms, provides a simple procedure for estimating ultimate lateral capacity of piles.

6. GROUP ACTION. Group action should be considered when the pile spacing in the direction of loading is less than 6 to 8 pile diameters. Group action can be evaluated by reducing the effective coefficient of lateral subgrade reaction in the direction of loading by a reduction factor R (Reference 9) as follows:

Pile Spacing in Direction of Loading D = Pile Diameter	Subgrade Reaction Reduction Factor R
8D	1.00
6D	0.70
4D	0.40
3D	0.25

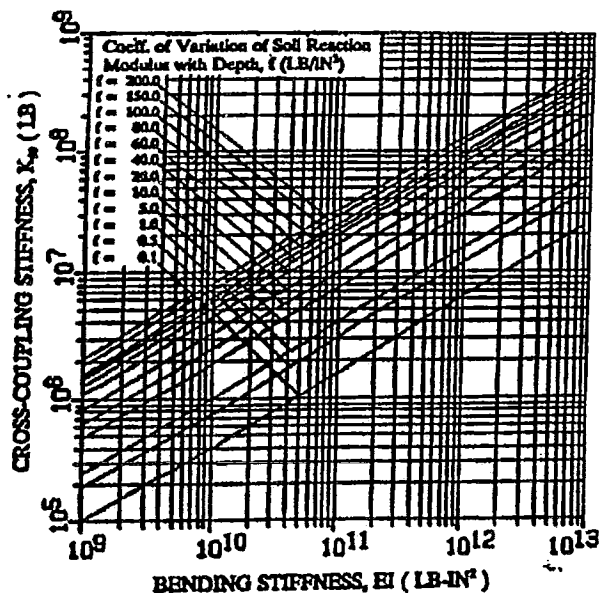


Figure 9. Pile Cross-Coupling Stiffness, K_{cc}

he authors. This recommendation and results of the correlation for clay are shown in Figure 11. Only the upper five lameters of soils (soil type and ground ster) need to be considered in usage of the presented design charts.

Limitations of Approach. There are several simplifying assumptions in the presented approach. The coefficient f is not an intrinsic soil parameter. The recommendations for f presented in Figures 9 and 11 are appropriate for piles in typical highway bridge foundations (i.e. smaller piles). Furthermore, the embedment effect has not been taken into account in the procedure. Therefore the recommendations are conservative and appropriate for shallow embedment conditions (say less than feet or 1.5 m).

Although correlations for the coefficient f can be conducted for other conditions (e.g. larger piles and bigger embedment apths), the additional complexity negates the merits of the use of simplified linear elastic solutions. For such cases, computer solutions, which can readily accommodate nonlinear effects and more general boundary conditions, are recommended.

Comparison to Caltrans Practice. The above procedure can be compared to the practice adopted by Caltrans. In Caltrans

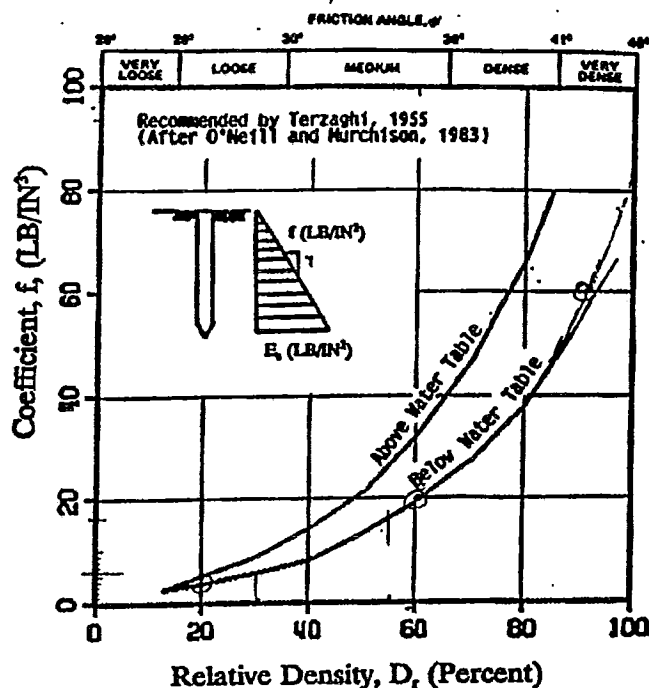


Figure 10. Recommendations for Coefficient f for Sands
(Note: 1 LB/IN³ = 0.27 N/cm³)

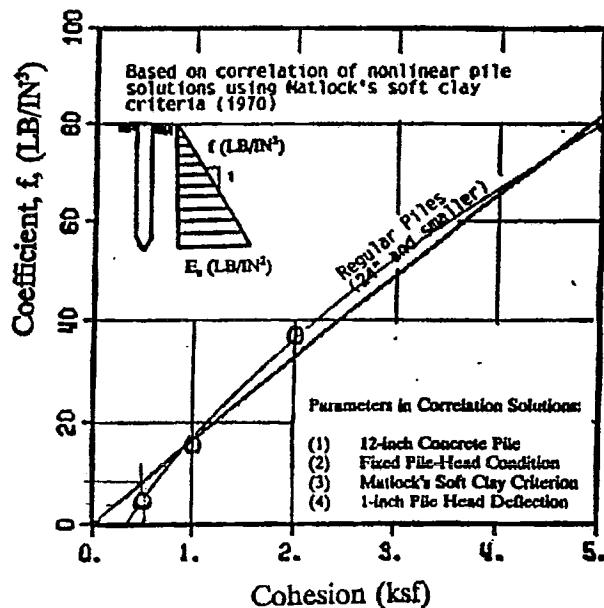


Figure 11. Recommendations of Coefficient f for Clays
(Note: 1 LB/IN³ = 0.27 N/cm³)